CMB Foregrounds: most recent set of Planck results and implications for the future of polarization measurements

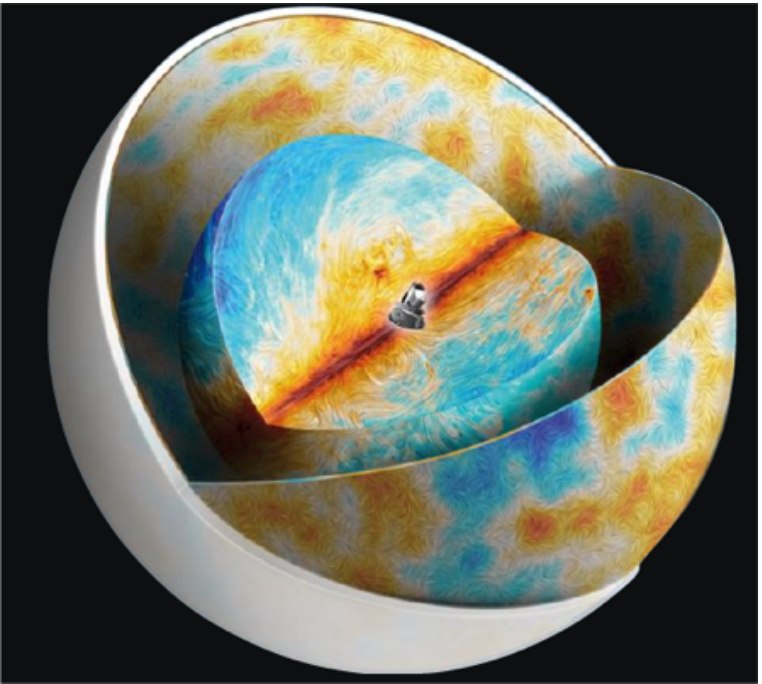

Tuhin Ghosh
(NISER Bhubaneswar)
On behalf of the Planck Collaboration
15th Rencontres du Vietnam Cosmology
August 12, 2019

CMB Foregrounds

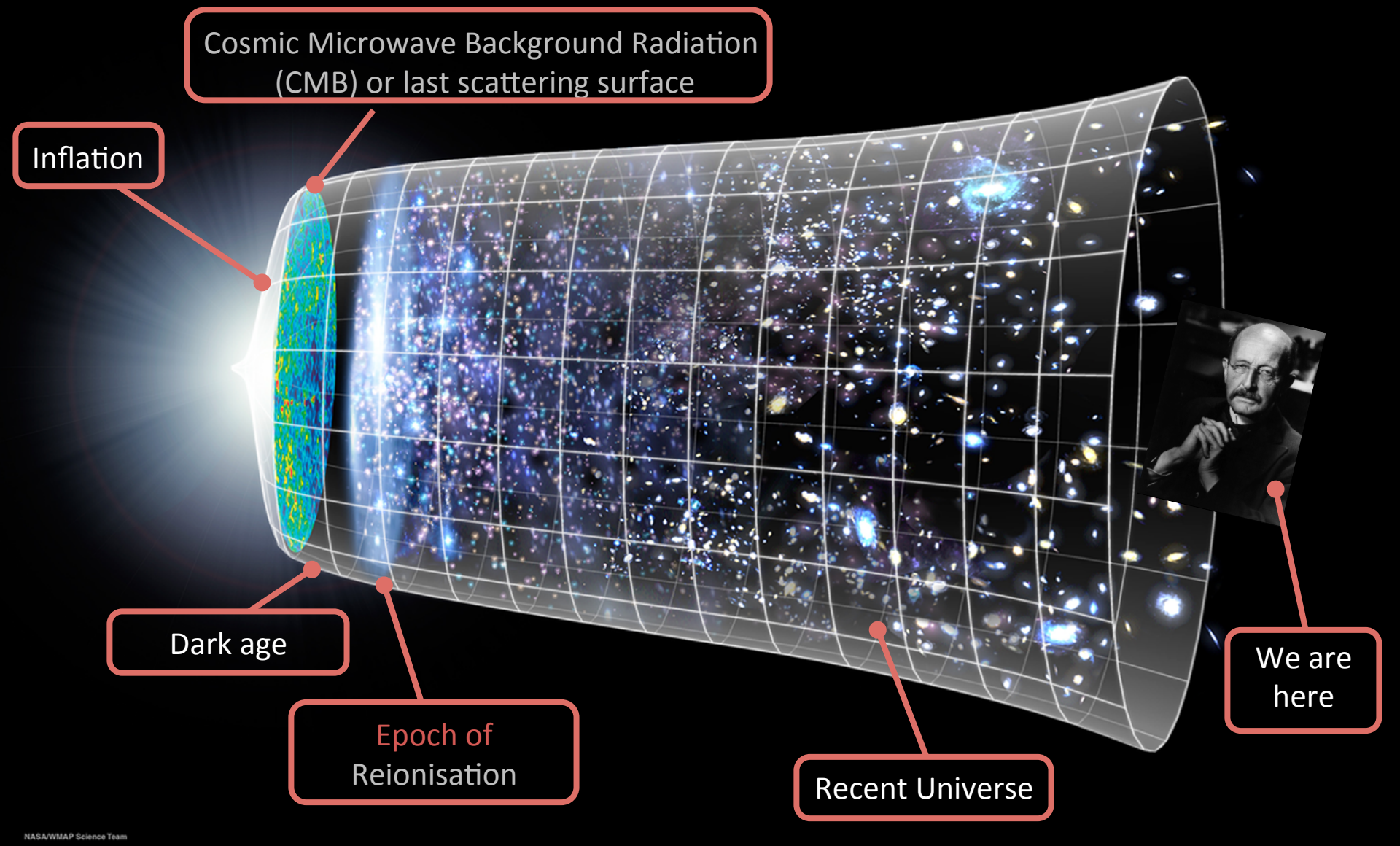

Foregrounds are everything between the CMB (last scattering surface) and the detectors

✧ Primary scientific goal:

To measure the temperature anisotropies of the CMB to fundamental limits down to angular resolution of 5arcmin; also measure polarization better than ever before

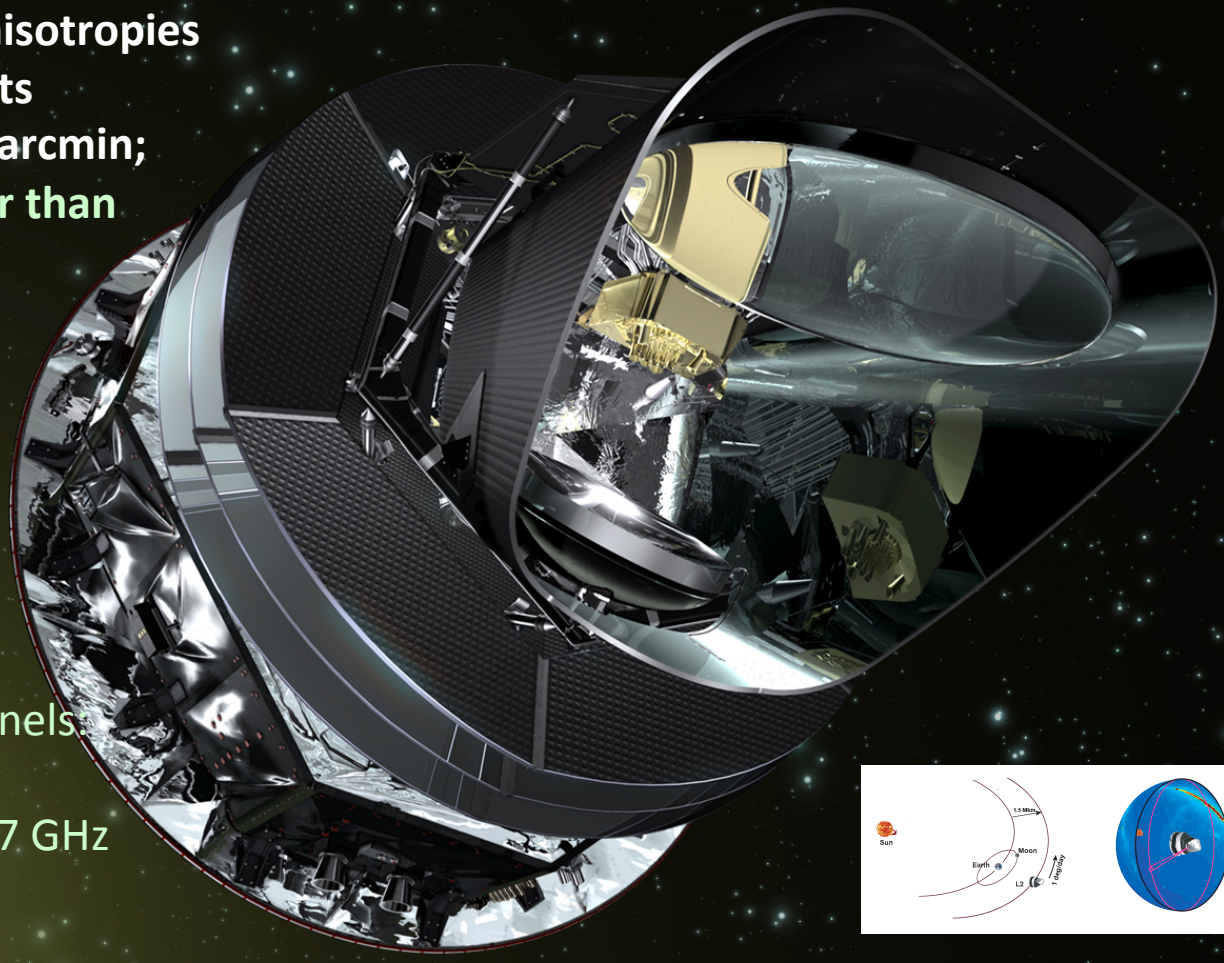

✧ Fly at Sun-Earth **L2** point

✧ Carry two instruments:

- Low Frequency Instrument (LFI), 20-K cryogenic amplifiers
- High Frequency Instrument (HFI), 0.1-K bolometers

✧ Observe at 9 frequency channels:

LFI - 30, 44, 70 GHz, and

HFI - 100, 143, 217, 353, 545, 857 GHz

to deal with foregrounds

Planck is the 3rd Generation Space CMB Mission

- Formally: "ESA mission with significant participation of NASA"

2018 maps

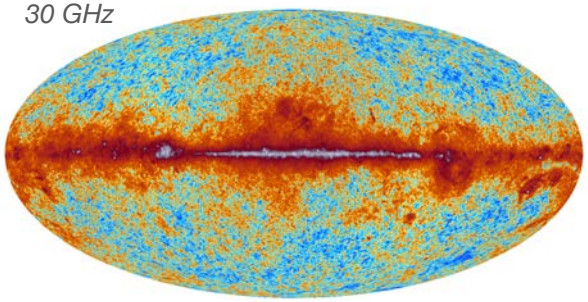
30 GHz

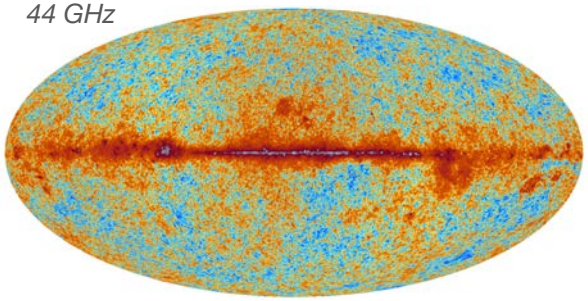
44 GHz

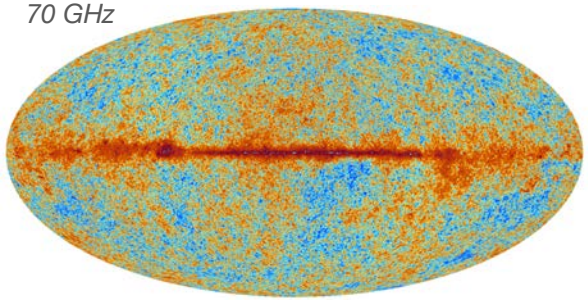
70 GHz

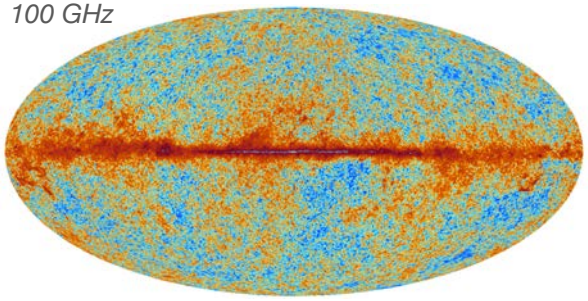
100 GHz

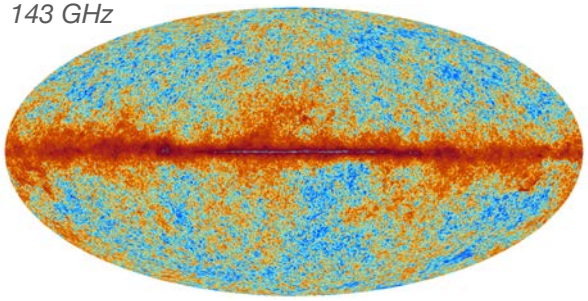
143 GHz

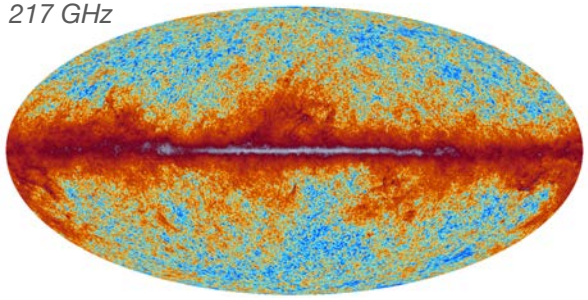
217 GHz

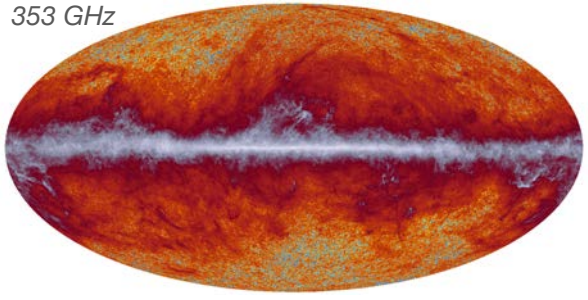
353 GHz

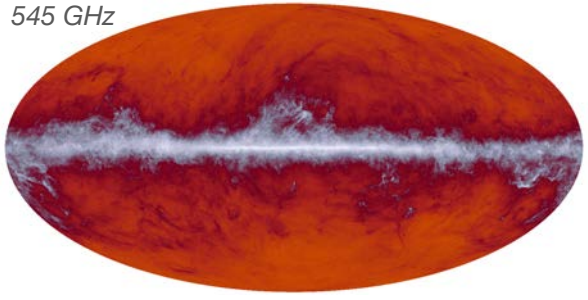
545 GHz

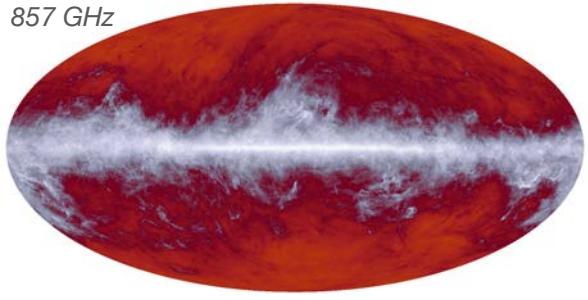
857 GHz

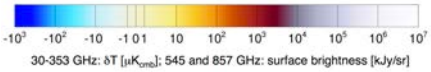
-10^3 -10^2 -10 -1 0 1 10 10^2 10^3 10^4 10^5 10^6 10^7
30-353 GHz: δT [μK_CMB]; 545 and 857 GHz: surface brightness [kJy/sr]

Diffuse temperature foregrounds at a glance

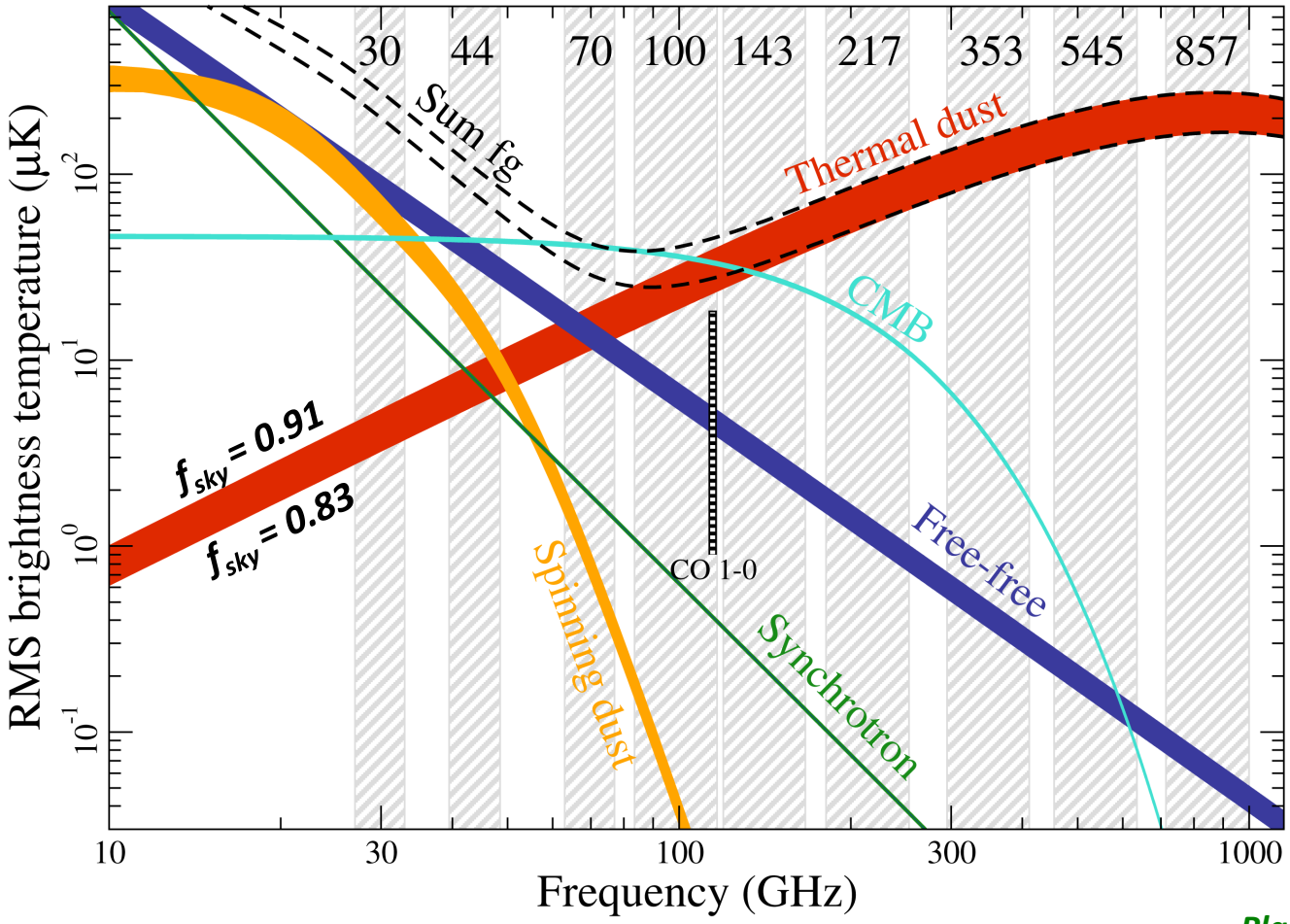

Temperature foreground minimum between **70 and 90 GHz** for sky fractions between 83 and 91% at **1 degree** resolution

Planck 2015 results X

Temperature foregrounds

Name	Description	Frequencies (GHz)	How to study it/ remove it
Synchrotron	Relativistic electrons in B-field	< 30	Radio surveys
Free-free	Electrons accelerated in ionized gas	< 100	Radio surveys/ recombination lines
Anomalous microwave emission (AME)	Electric dipole radiation from small spinning dust grains	10 - 100	Microwave surveys
Thermal dust	Blackbody radiation from warm dust (T ~10-30 K)	> 100	Submm/IR surveys & UV/ optical
Line contamination	Atomic and Molecular lines (e.g. CO)	Various	Spectroscopic surveys/split bands
Radio sources	Synchrotron emission from AGN	< 150	High resolution radio surveys
Dusty galaxies	Dust emission from dusty galaxies	> 150	High resolution sub-mm/IR surveys
CIB	Integrated emission from high z galaxies	> 100	High resolution sub-mm/IR surveys
SZ (clusters)	Inverse Compton scattering of CMB photons off hot electrons in IGM	10 - 300	High resolution CMB surveys
Zodiacal light	Dust emission from solar system cloud	> 100	Submm/IR surveys

Commander foreground model

Table 4. Summary of main parametric signal models for the temperature analysis.

Component	Free parameters and priors	Brightness temperature, s_ν [μK$_{\rm RJ}$]	Additional information
CMB[a]	$A_{\rm cmb} \sim {\rm Uni}(-\infty, \infty)$	$x = \frac{h\nu}{k_{\rm B} T_{\rm CMB}}$ $g(\nu) = (\exp(x)-1)^2/(x^2\exp(x))$ $s_{\rm CMB} = A_{\rm CMB}/g(\nu)$	$T_{\rm CMB} = 2.7255$ K
Synchrotron[a] . . .	$A_{\rm s} > 0$ $\alpha > 0$, spatially constant	$s_{\rm s} = A_{\rm s}\left(\frac{\nu_0}{\nu}\right)^2 \frac{f_{\rm s}(\frac{\nu}{\alpha})}{f_{\rm s}(\frac{\nu_0}{\alpha})}$	$\nu_0 = 408$ MHz $f_{\rm s}(\nu) =$ Ext template
Free-free	$\log {\rm EM} \sim {\rm Uni}(-\infty, \infty)$ $T_{\rm e} \sim N(7000 \pm 500\,{\rm K})$	$g_{\rm ff} = \log\left\{\exp\left[5.960 - \sqrt{3}/\pi \log(\nu_9\ T_4^{-3/2})\right] + e\right\}$ $\tau = 0.05468\ T_{\rm e}^{-3/2}\ \nu_9^{-2}\ {\rm EM}\ g_{\rm ff}$ $s_{\rm ff} = 10^6\, T_{\rm e}\,(1 - e^{-\tau})$	$T_4 = T_{\rm e}/10^4$ $\nu_9 = \nu/(10^9\ {\rm Hz})$
Spinning dust . . .	$A^1_{\rm sd}, A^2_{\rm sd} > 0$ $\nu^1_{\rm p} \sim N(19 \pm 3\,{\rm GHz})$ $\nu^2_{\rm p} > 0$, spatially constant	$s_{\rm sd} = A_{\rm sd} \cdot \left(\frac{\nu_0}{\nu}\right)^2 \frac{f_{\rm sd}(\nu\cdot\nu_{\rm p0}/\nu_{\rm p})}{f_{\rm sd}(\nu_0\cdot\nu_{\rm p0}/\nu_{\rm p})}$	$\nu^1_0 = 22.8$ GHz $\nu^2_0 = 41.0$ GHz $\nu_{\rm p0} = 30.0$ GHz $f_{\rm sd}(\nu) =$ Ext template
Thermal dust[a] . .	$A_{\rm d} > 0$ $\beta_{\rm d} \sim N(1.55 \pm 0.1)$ $T_{\rm d} \sim N(23 \pm 3\,{\rm K})$	$\gamma = \frac{h}{k_{\rm B} T_{\rm d}}$ $s_{\rm d} = A_{\rm d} \cdot \left(\frac{\nu}{\nu_0}\right)^{\beta_{\rm d}+1} \frac{\exp(\gamma\nu_0)-1}{\exp(\gamma\nu)-1}$	$\nu_0 = 545$ GHz
SZ	$y_{\rm sz} > 0$	$s_{\rm sz} = 10^6\, y_{\rm sz}/g(\nu)\, T_{\rm CMB}\left(\frac{x(\exp(x)+1)}{\exp(x)-1} - 4\right)$	
Line emission . .	$A_i > 0$ $h_{ij} > 0$, spatially constant	$s_i = A_i h_{ij} \frac{F_i(\nu_j)}{F_i(\nu_0)} \frac{g(\nu_0)}{g(\nu_j)}$	$i \in \begin{cases} {\rm CO}\ J=1\rightarrow 0 \\ {\rm CO}\ J=2\rightarrow 1 \\ {\rm CO}\ J=3\rightarrow 2 \\ 94/100 \end{cases}$ $j =$ detector index $F =$ unit conversion

Notes. For polarization, the same parametric functions are employed, but only CMB, synchrotron, and thermal dust emission are included in the model, with spectral parameters fixed to the result of the temperature analysis. The symbol "~" implies that the respective parameter has a prior as given by the right-hand side distribution; Uni denotes a uniform distribution within the indicated limits, and N denotes a (normal) Gaussian distribution with the indicated mean and standard devation. [(a)] Polarized component.

Planck 2015 results X

Temperature sky model

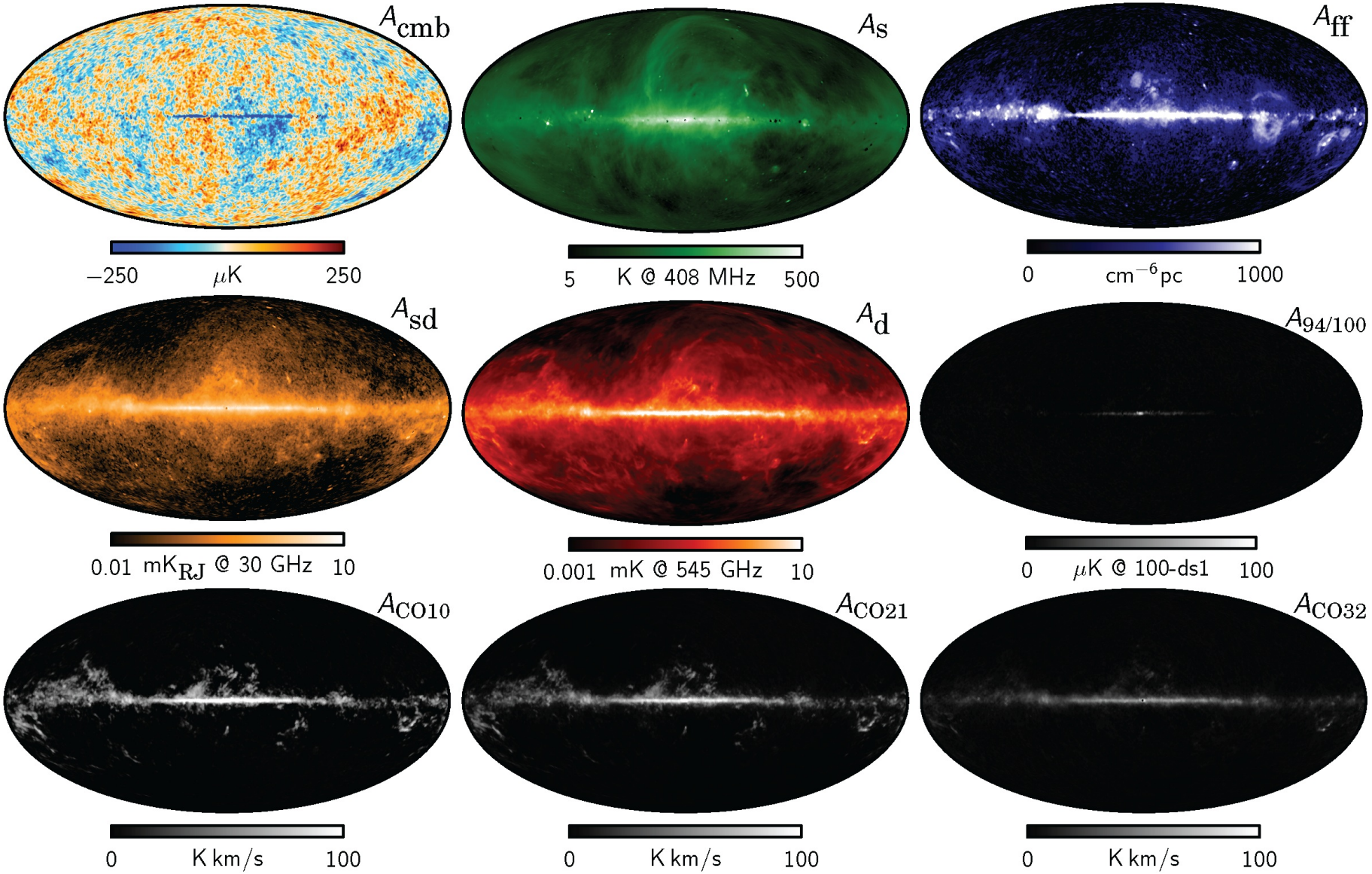

Planck 2015 results X

Polarized galactic **synchrotron** dominates at low frequencies

Planck polarized maps at seven frequencies

Polarized thermal emission (~20K) from galactic **dust** aligned in magnetic fields dominates at high frequencies

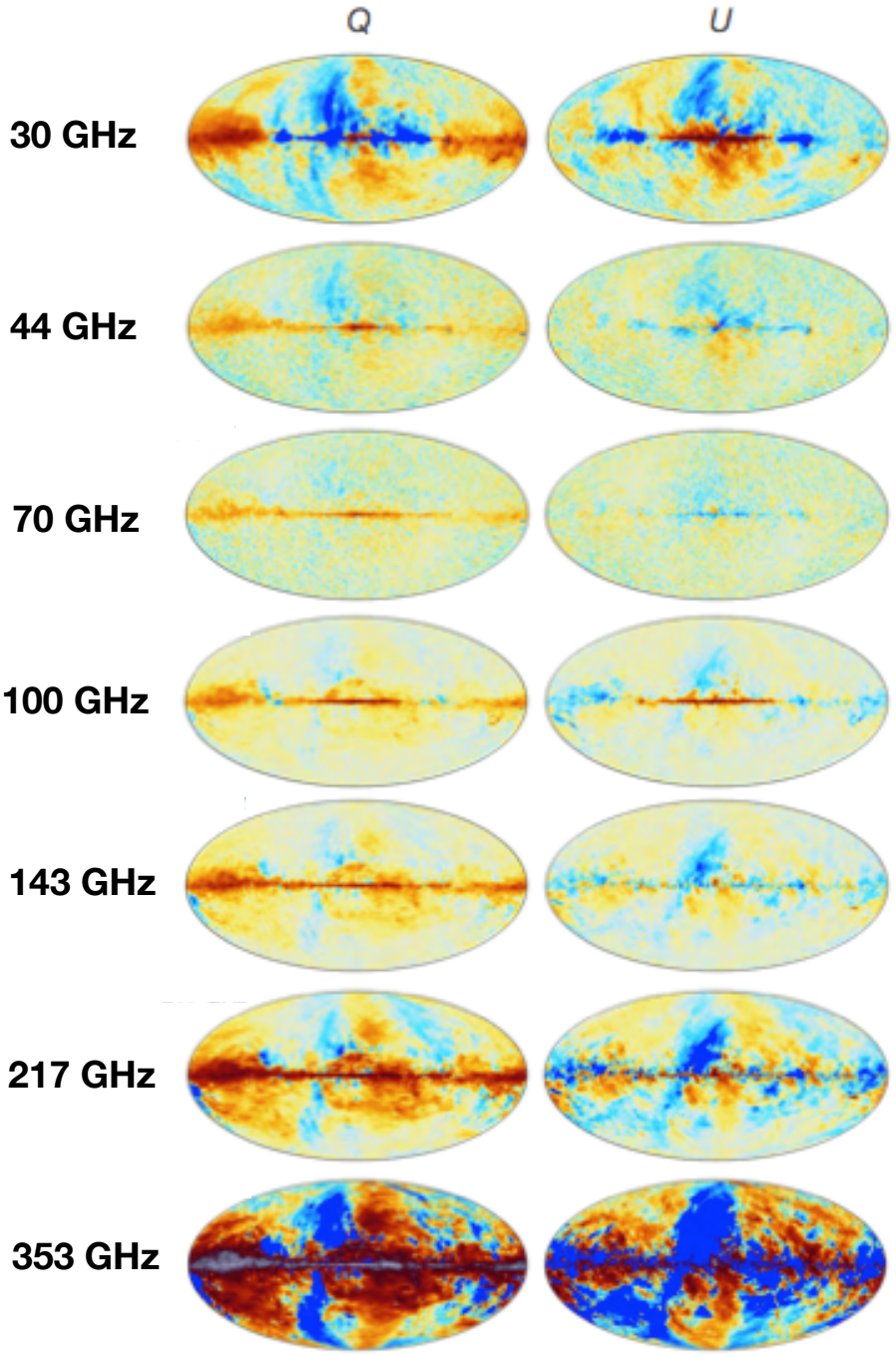

Planck 2018 results I

HFI: 2015 odd-even surveys

1. null test: (odd-even) surveys are scanned in opposite direction
2. this reveals time constant and far side lobes residual effects

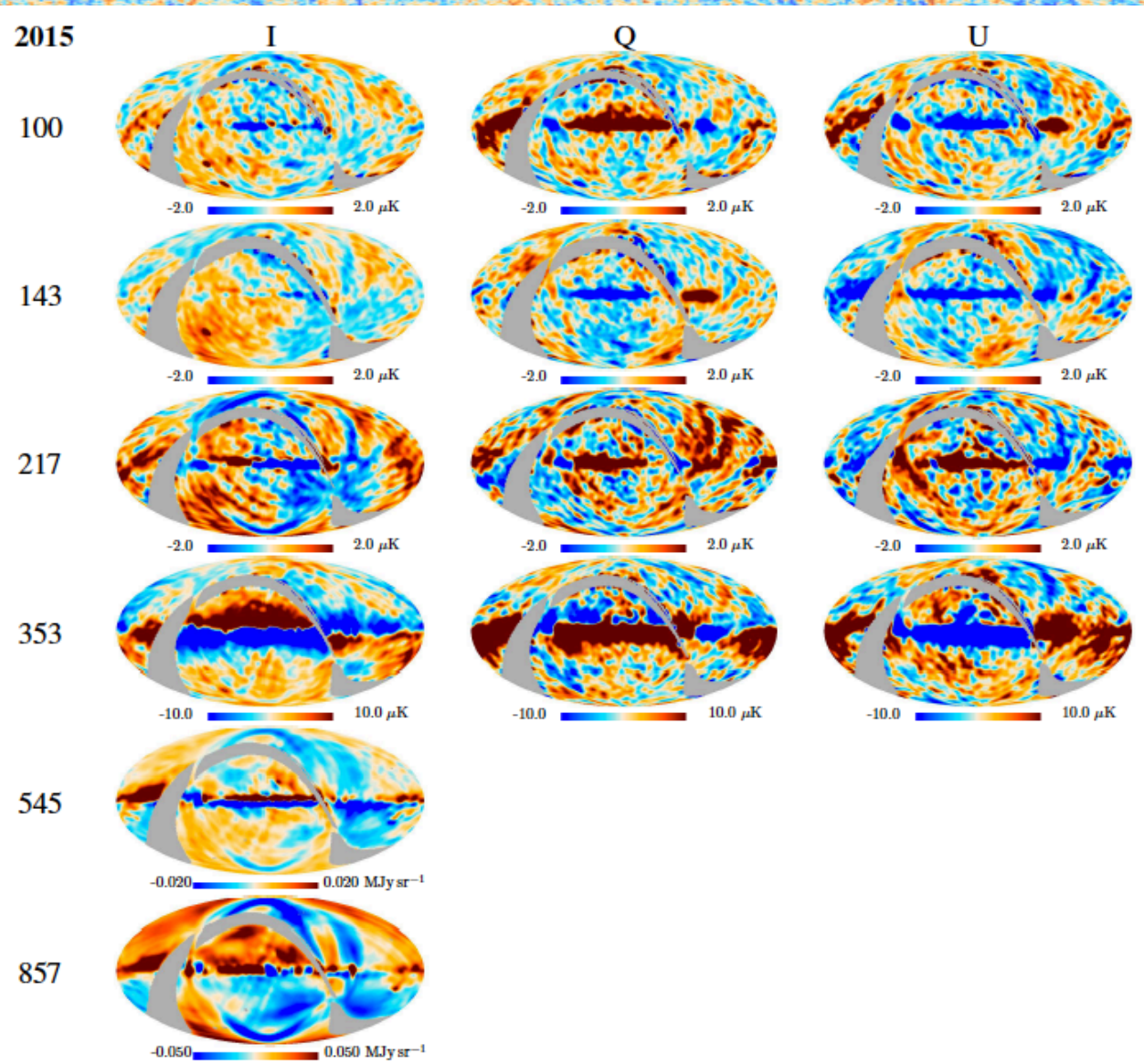

HFI: 2018 odd-even surveys

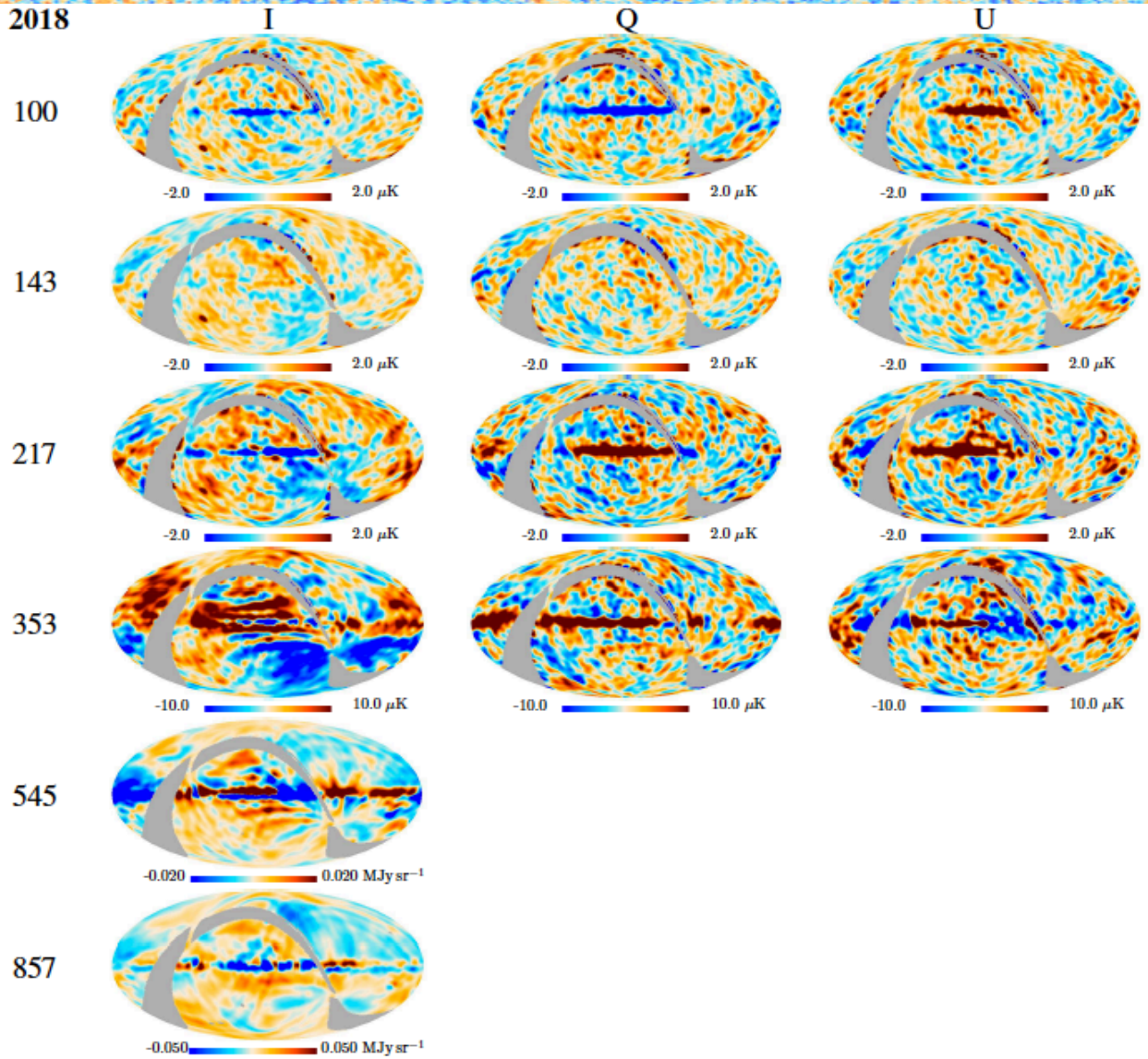

Polarized foregrounds

Name	Polarization fraction	Spectral distribution	Spatial distribution	Statistical distribution
CMB	< 10%	Black-body	Described by Cosmology	Gaussian
Synchrotron	upto 75 %	Power-law with spectral index = -3.0	$\propto \ell^{-2.7}$	Highly non-Gaussian
Thermal dust	~ 20%	Modified black body with T ~ 20 K and spectral index ~ 1.6	$\propto \ell^{-2.4}$	Highly non-Gaussian
AME	unknown upto few %	-	-	Highly non-Gaussian
CO Line contamination	upto 10% in molecular clouds	-	$\propto \ell^{-3}$?	Highly non-Gaussian, concentrated on molecular clouds

Polarization sky model

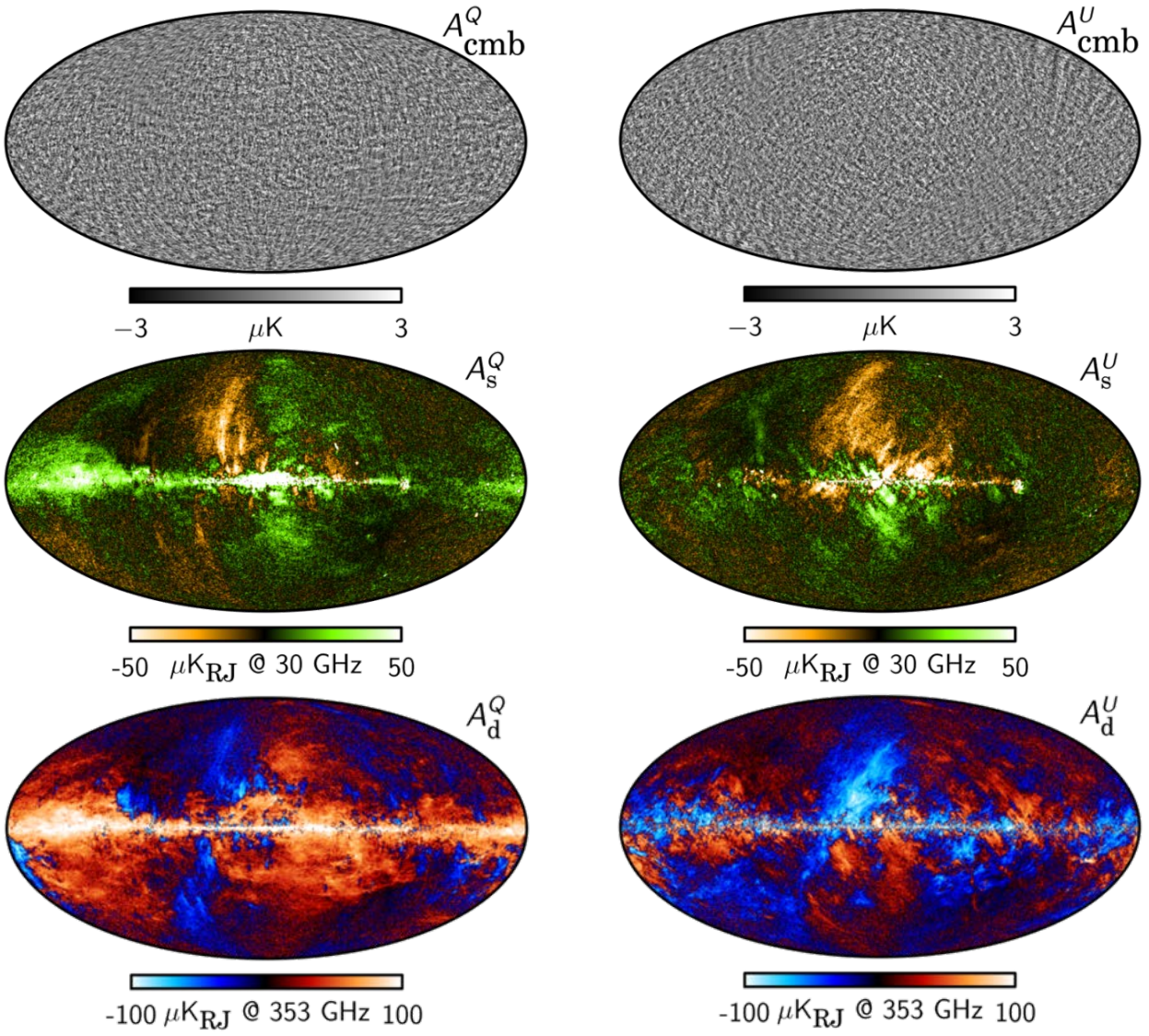

Planck 2015 results X

Ignoring foregrounds can bias the CMB B-mode signal

Inaccurate modelling of dust

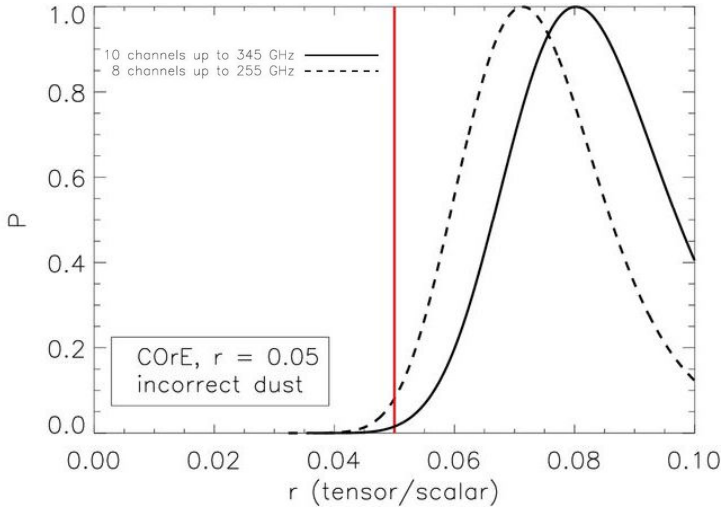

Ignoring synchrotron curvature

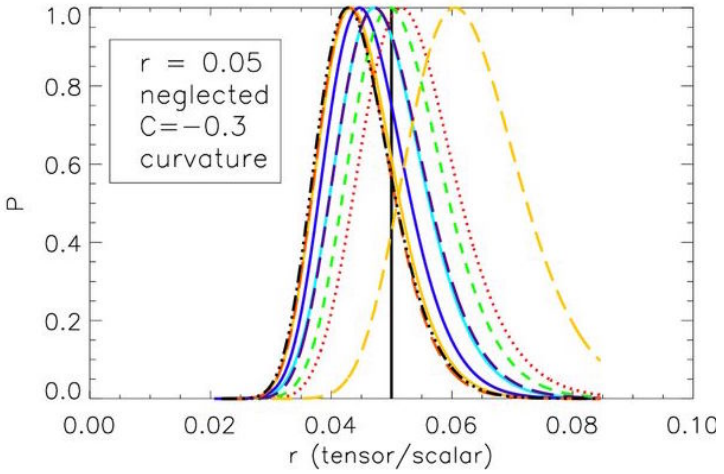

Inaccurate modelling of dust

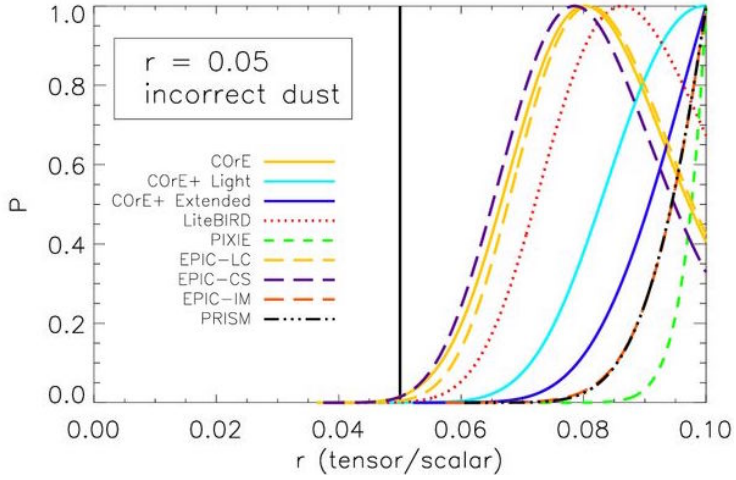

Ignoring 1% spinning dust

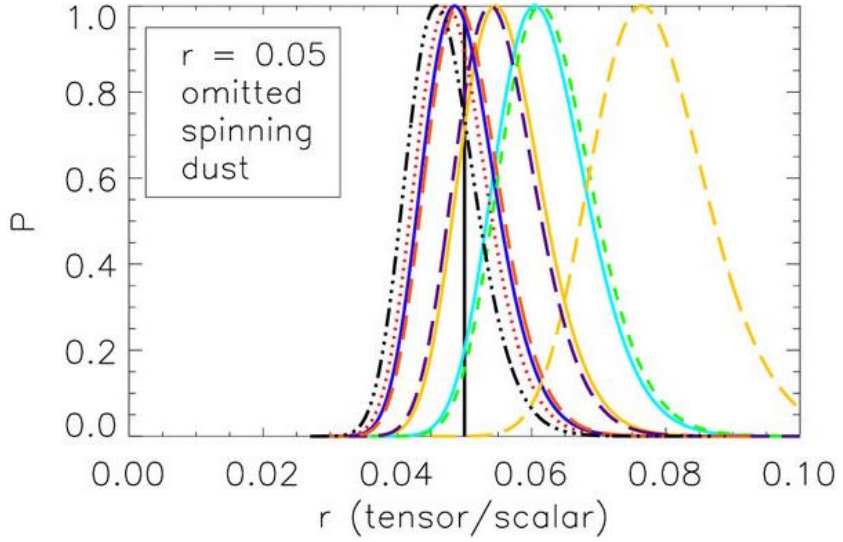

Remazeilles et al. 2016

Polarized synchrotron emission

- Relativistic cosmic ray electrons accelerating in Galactic magnetic field
- Dominates polarised sky up to 80 GHz
- Up to 70% polarised (theoretically)
  ~40-50% max observed
  ~20% typical
- Steep spectrum **β ~ -3.13 +/- 0.13**
- Low frequencies (< few GHz) corrupted by Faraday Rotation
- WMAP 23 GHz/Planck 28.5 GHz only good templates so far

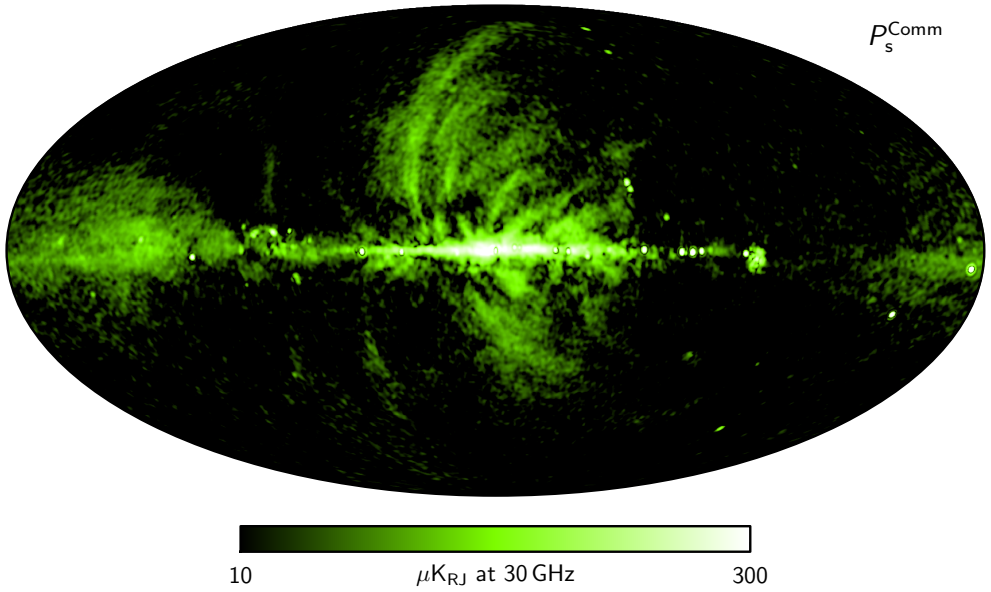

Polarized synchrotron emission

- Large-scale power from Galactic plane and several “loops/spurs”
  - Highly polarised
  - Cover large fraction of the sky!
  - May be responsible for bulk of synchrotron radiation!

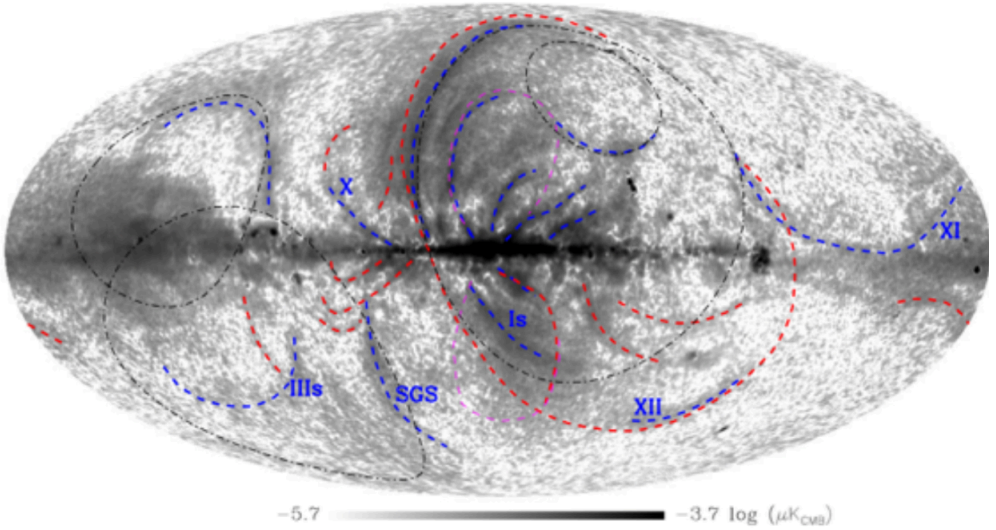

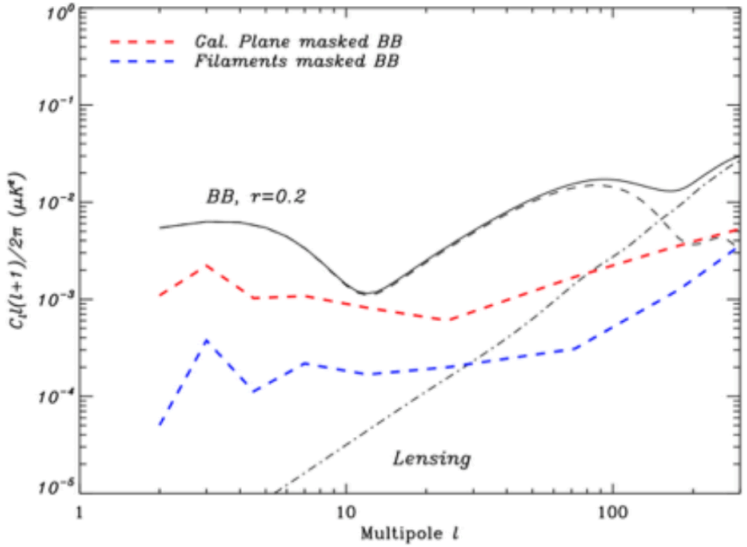

Vidal et al. (2015)

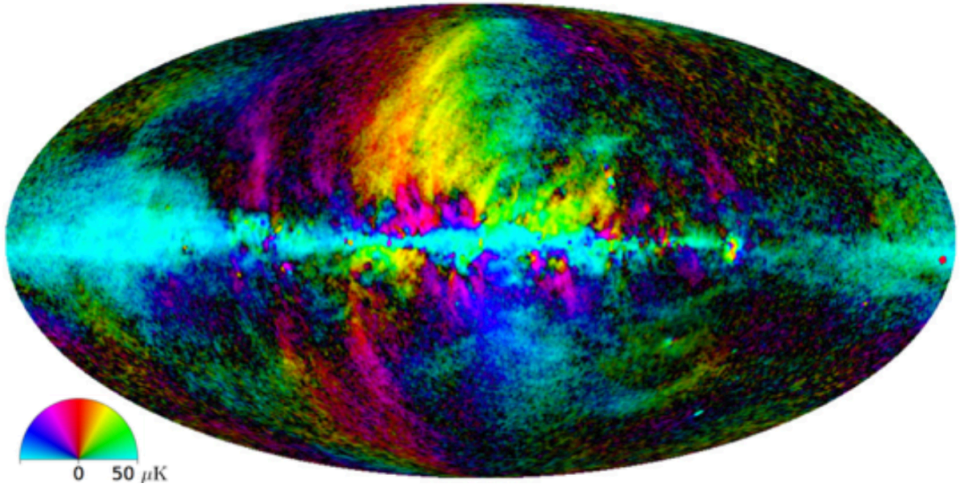

Planck Collaboration, 2015, arXiv:1506.06660

Synchrotron SED combining SPASS and Planck/WMAP

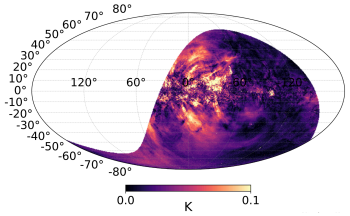

$$D_\ell(\nu_1 \times \nu_2) = A_s \left(\frac{\nu_1}{\nu_0}\right)^{\beta_s + s_{run}\log(\nu_1/\nu_0)} \left(\frac{\nu_2}{\nu_0}\right)^{\beta_s + s_{run}\log(\nu_2/\nu_0)}$$

Krachmalnicoff et al. 2018

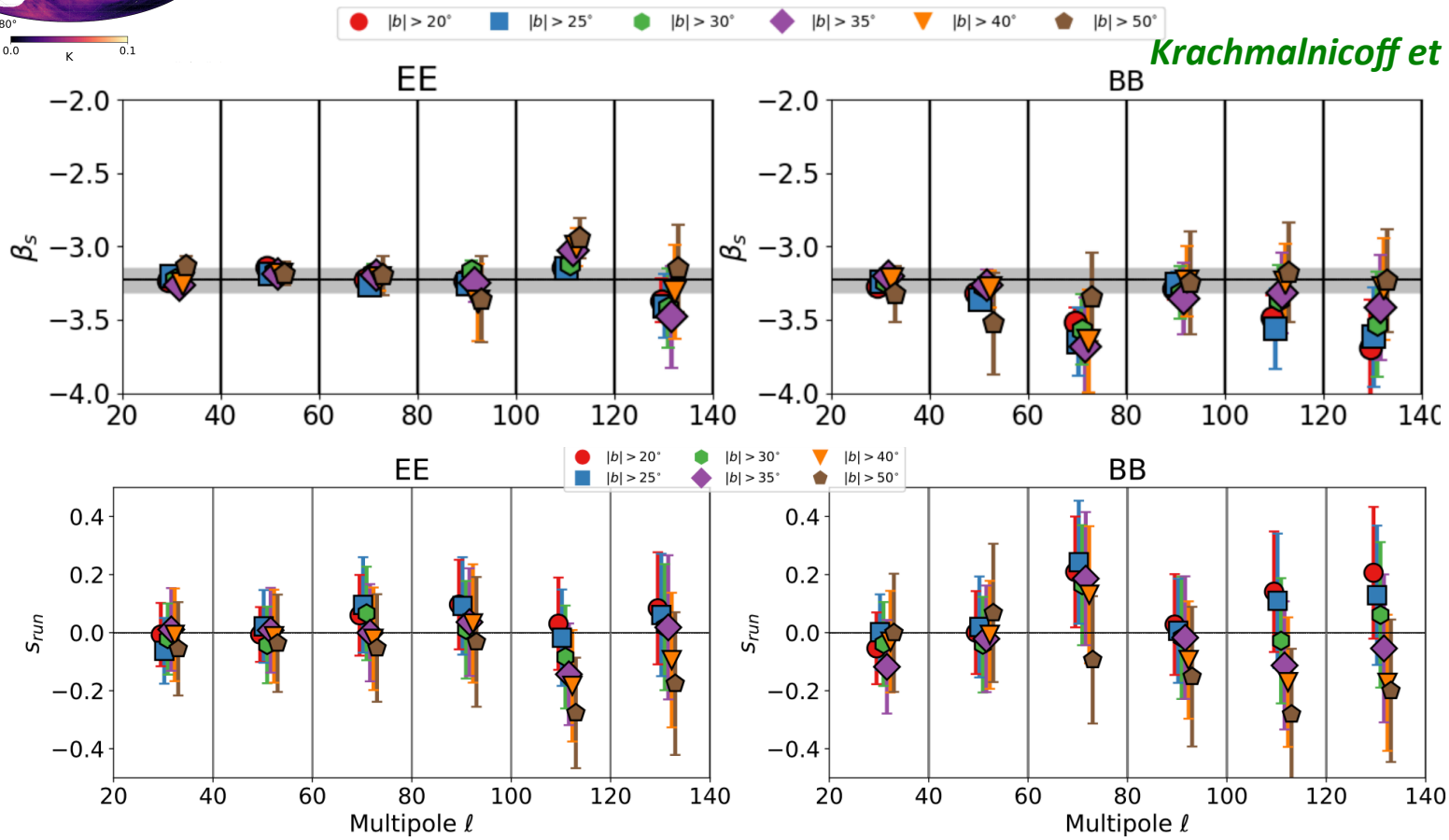

- Strong degeneracy between β_s and s_{run}
- **Gaussian prior on spectral index** from WMAP and Planck: $\beta_s = -3.13 \pm 0.13$
- s_{run} **compatible with zero**, with 1σ errors between 0.07 and 0.14

Anomalous Microwave Emission (AME)

- The AME arises from rapidly spinning ultrasmall grains (i.e. nanoparticles < 10 nm)
- The exact carrier is unknown: spinning Polycyclic Acromatic Hydrocarbon (PAH) may not be dominating, spinning silicate nanoparticles are promising candidates.
- The polarization of AME is uncertain: polarization of spinning PAH is small (depends on the magnetic field strength), but polarization of spinning nanosilicates can be large.

Spinning PAH

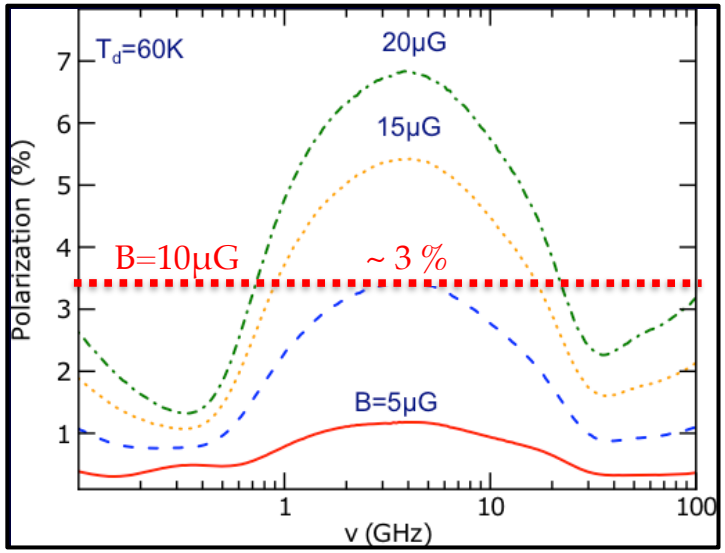

Hoang and Lazarian 2015

Spinning nanosilicates

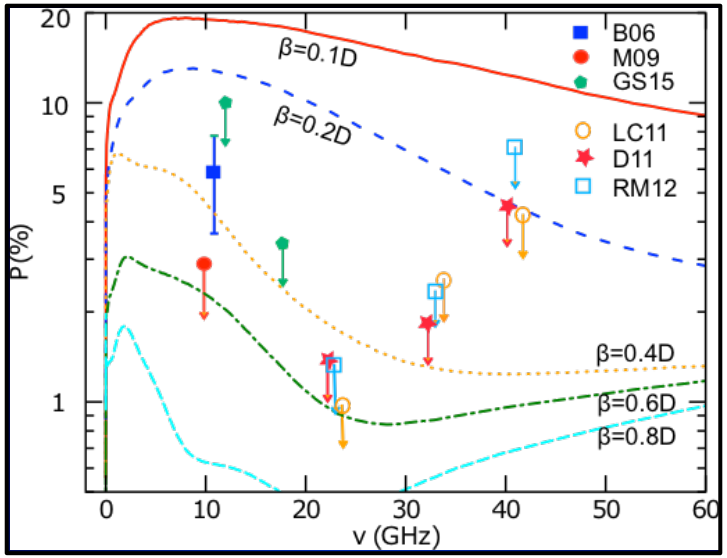

Hoang et al. 2016

Hensley et al. 2016 find no correlation between AME and PAH abundance by comparing *Planck* AME map and WISE data.

Future observations are needed to constrain the alignment of the nanoparticles with the magnetic field.

Physics of dust polarization

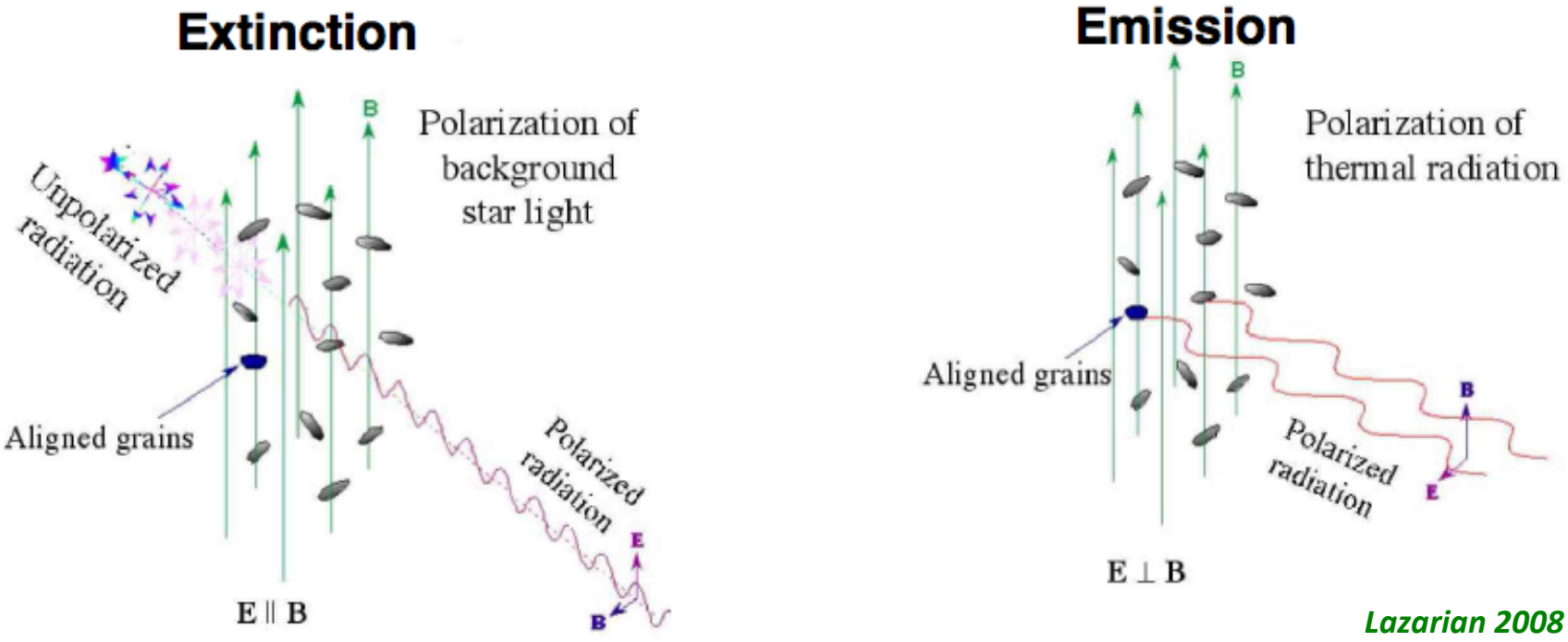

Lazarian 2008

Galactic dust polarization traces:

- the structure of the Galactic magnetic field
- the alignment mechanisms and efficiency
- the nature of the dust grains

Dust emission is a major polarized foreground to CMB B-modes

Polarized foregrounds

reionization B-modes

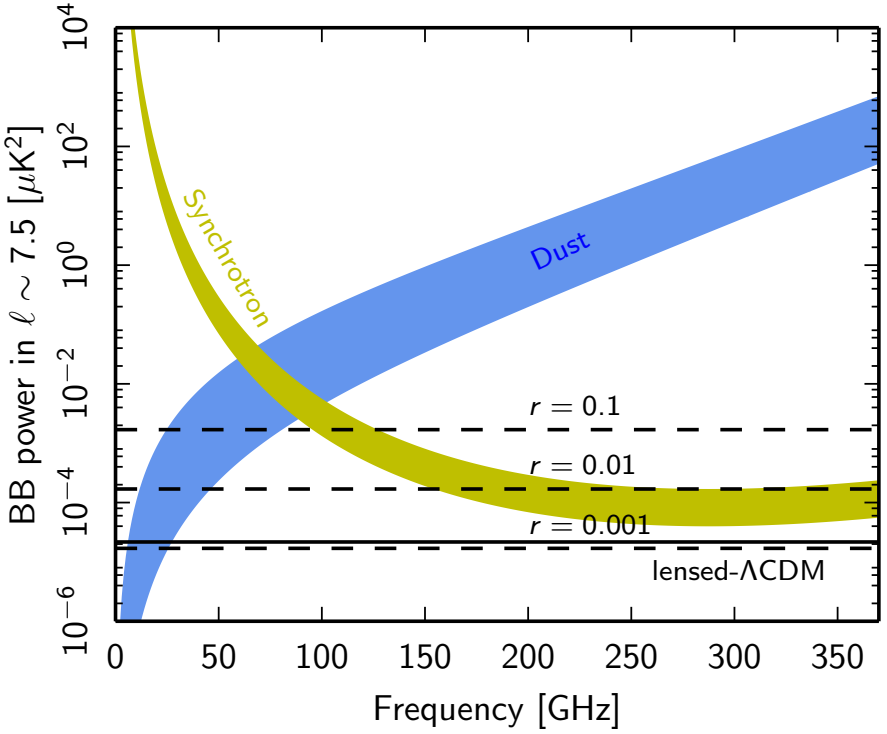

recombination B-modes

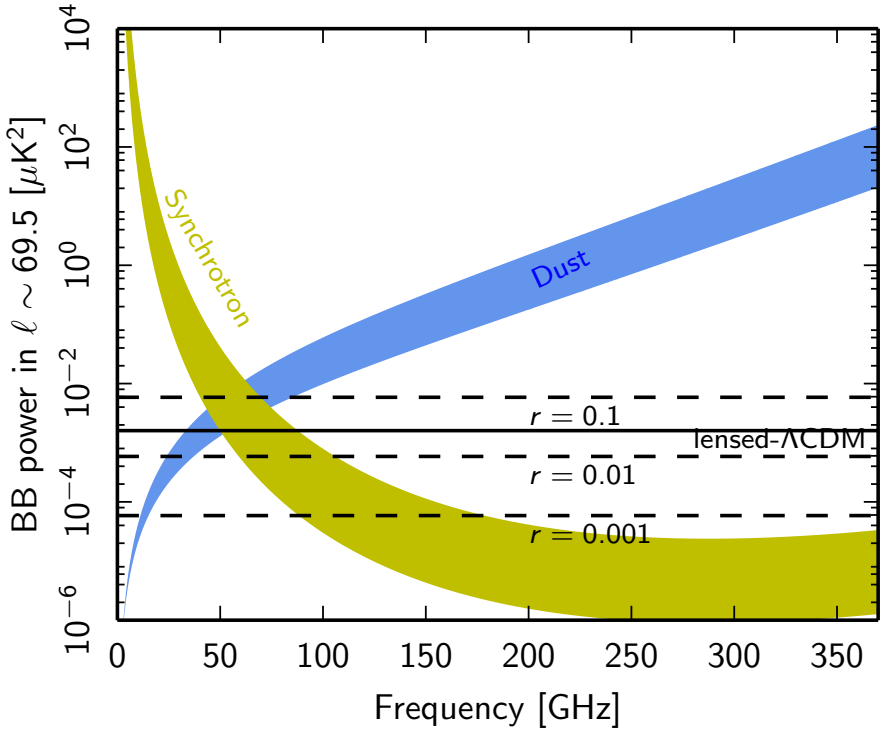

- The frequency at which dust and synchrotron *B*-modes power are equal depends on multipole and sky region.
- Dust quickly dominates synchrotron at higher frequencies.

Polarized foregrounds

E-mode signal

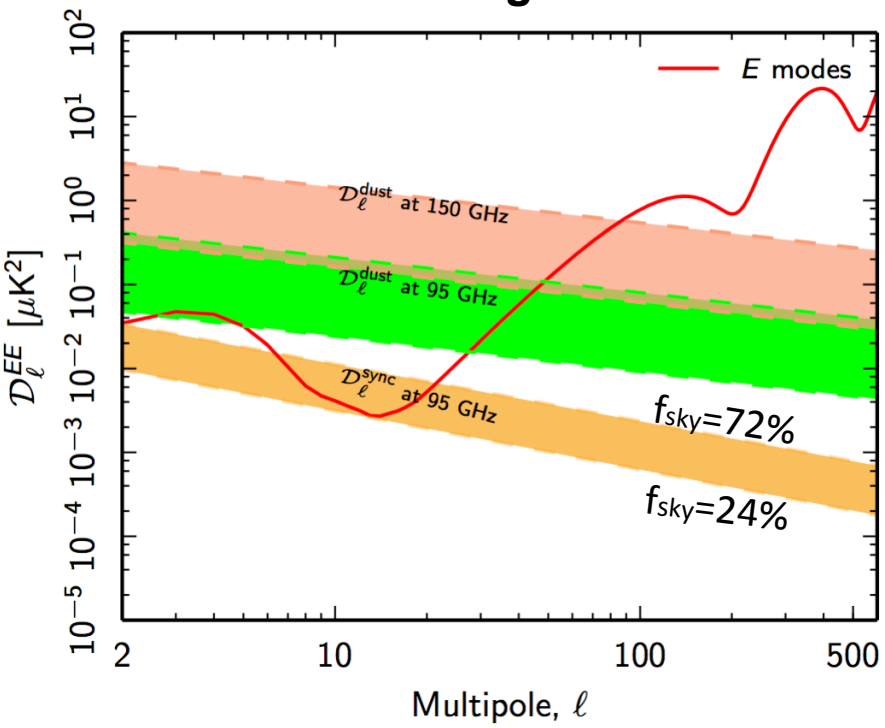

B-mode signal

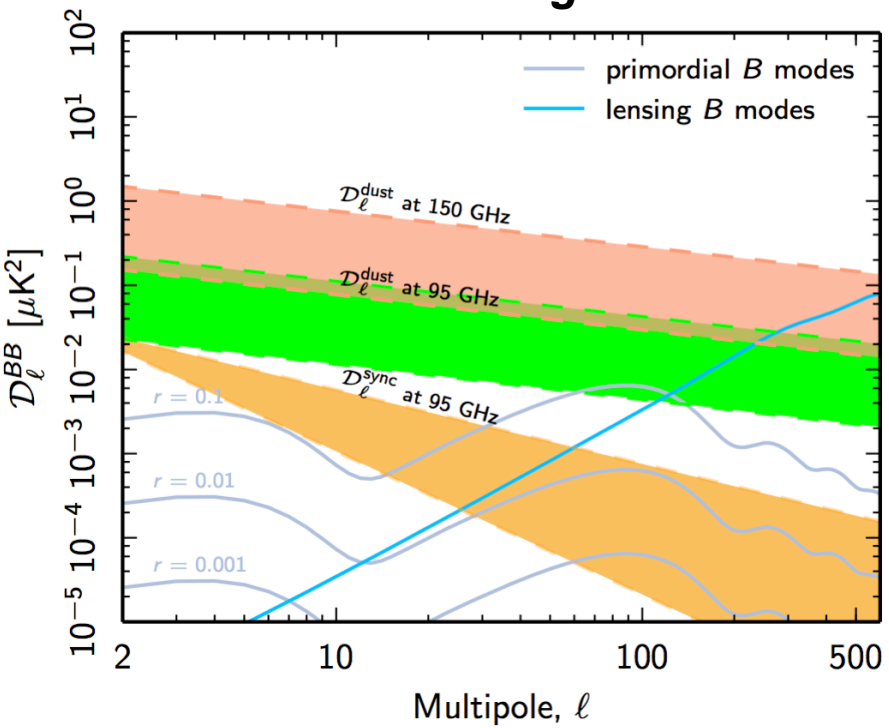

Planck 2015 results X

Planck Intermediate results. XXX 2016

Polarized dust spectral indices at intermediate latitude sky

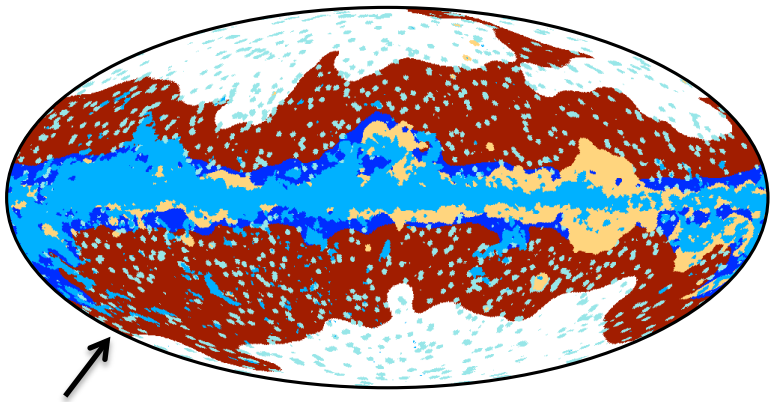

Only red sky region is considered

To characterize the polarized dust SED, we cross-correlate 353 GHz Q and U maps with the three lowest *Planck* HFI frequency channels (100 – 217 GHz) + LFI (30 – 70 GHz) + *WMAP* (23 – 94 GHz) in the pixel space.

$$\langle \beta^{\rm P}_{\rm d,mm} \rangle = 1.59 \pm 0.17, \; T_{\rm d} = 19.6 \; {\rm K}$$

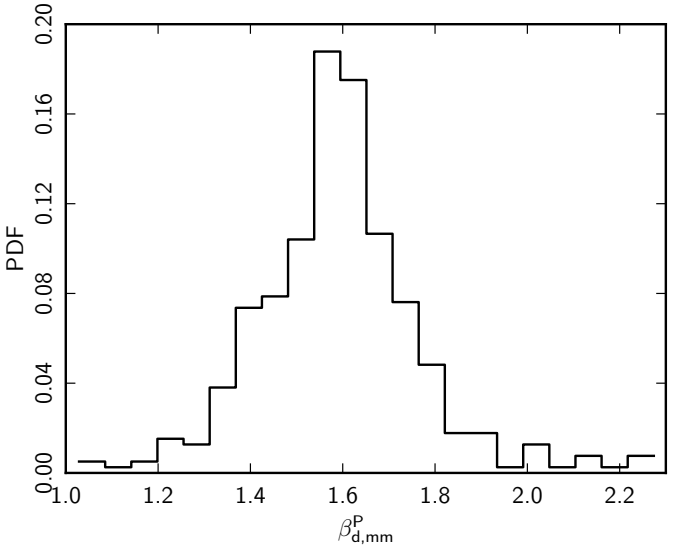

The cross-correlation coefficients at and above 100 GHz can be decomposed as

$$[\alpha^{\rm P}_{\nu}]^{\rm 1T}_{353} = \alpha^{P}(c_{353}) + \alpha^{\rm P}_{\nu}(d_{353})$$

We work with the colour ratio between two frequencies ν_1 and ν_2 (ν_0 is used as a reference to get rid of the CMB contribution)

$$\begin{aligned} R^{\rm P}_{\nu_0}(\nu_2,\nu_1) &= \frac{[\alpha^{\rm P}_{\nu_2}]^{1T}_{353} - [\alpha^{\rm P}_{\nu_0}]^{1T}_{353}}{[\alpha^{\rm P}_{\nu_1}]^{1T}_{353} - [\alpha^{\rm P}_{\nu_0}]^{1T}_{353}} \\ &= \frac{\alpha^{\rm P}_{\nu_2}(d_{353}) - \alpha^{\rm P}_{\nu_0}(d_{353})}{\alpha^{\rm P}_{\nu_1}(d_{353}) - \alpha^{\rm P}_{\nu_0}(d_{353})} \\ &= f(\beta_{\rm d}, T_{\rm d}) \end{aligned}$$

Planck intermediate results. XXII 2015

Polarized foregrounds SED

The cross-correlation coefficients are fitted with a simple two-component foreground model (dust + 353 GHz correlated synchrotron):

$$[\alpha_\nu^{\rm P}]^{\rm 1T}_{353} = A_{\rm s}\left(\frac{\nu_1}{23}\right)^{\beta_{\rm s}} + \left(\frac{\nu_1}{353}\right)^{\beta_{\rm d}-2}\frac{B_{\nu_1}(T_{\rm d})}{B_{353}(T_{\rm d})} \qquad T_{\rm d} = 19.6\,{\rm K}$$

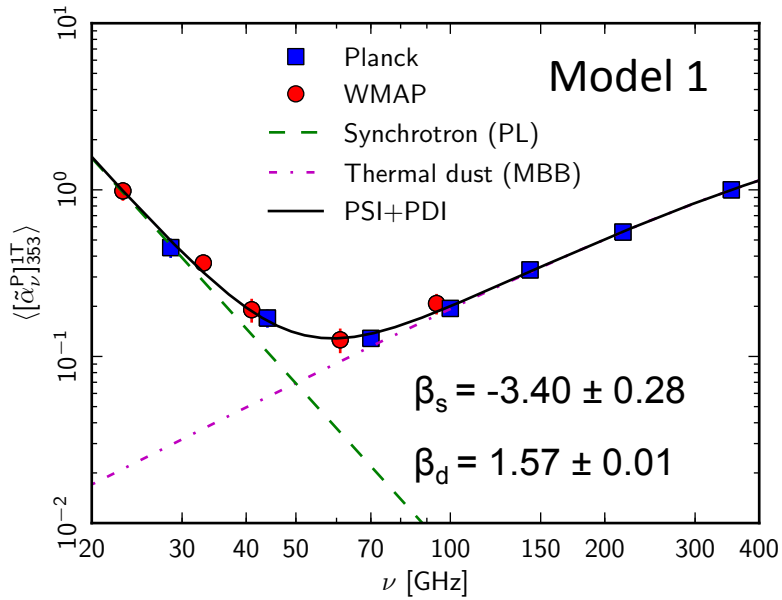

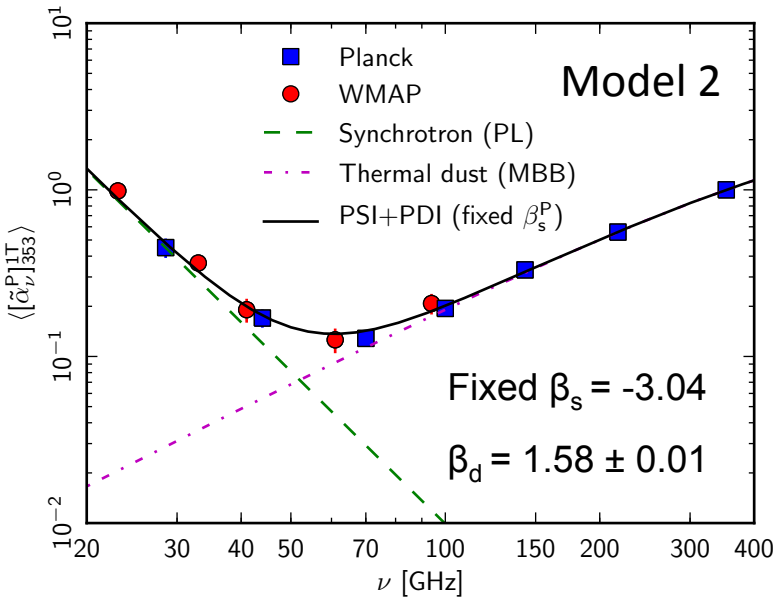

Issues:

Planck intermediate results. XXII 2015

- The template polarization maps at 353 GHz have low signal-to-noise ratio at high Galactic latitudes.
- Such correlation analysis picks up only 353-GHz correlated signal. The measured dust SED could be biased due to the spectral decorrelation.

Planck 2018 results: dust angular power spectra

Nested sky regions

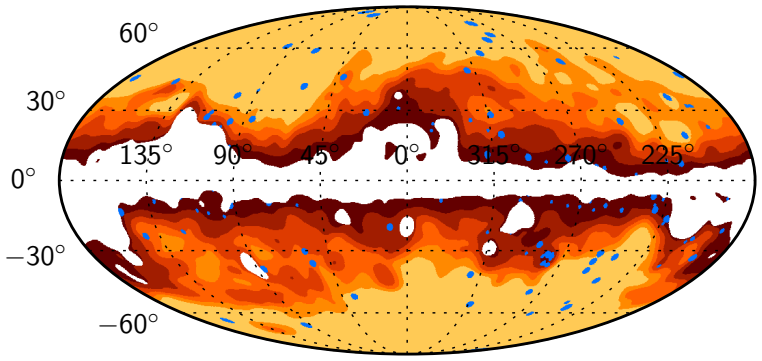

T-E correlation ratio

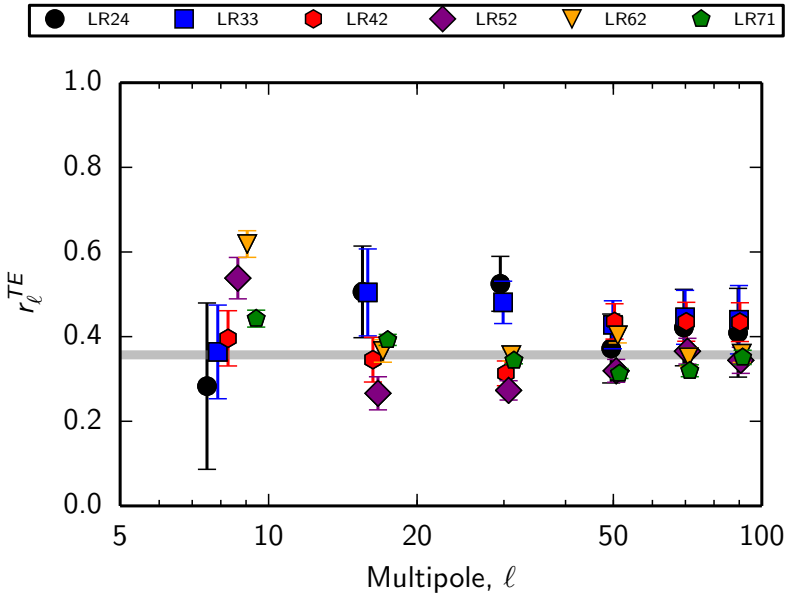

353 GHz angular power spectra

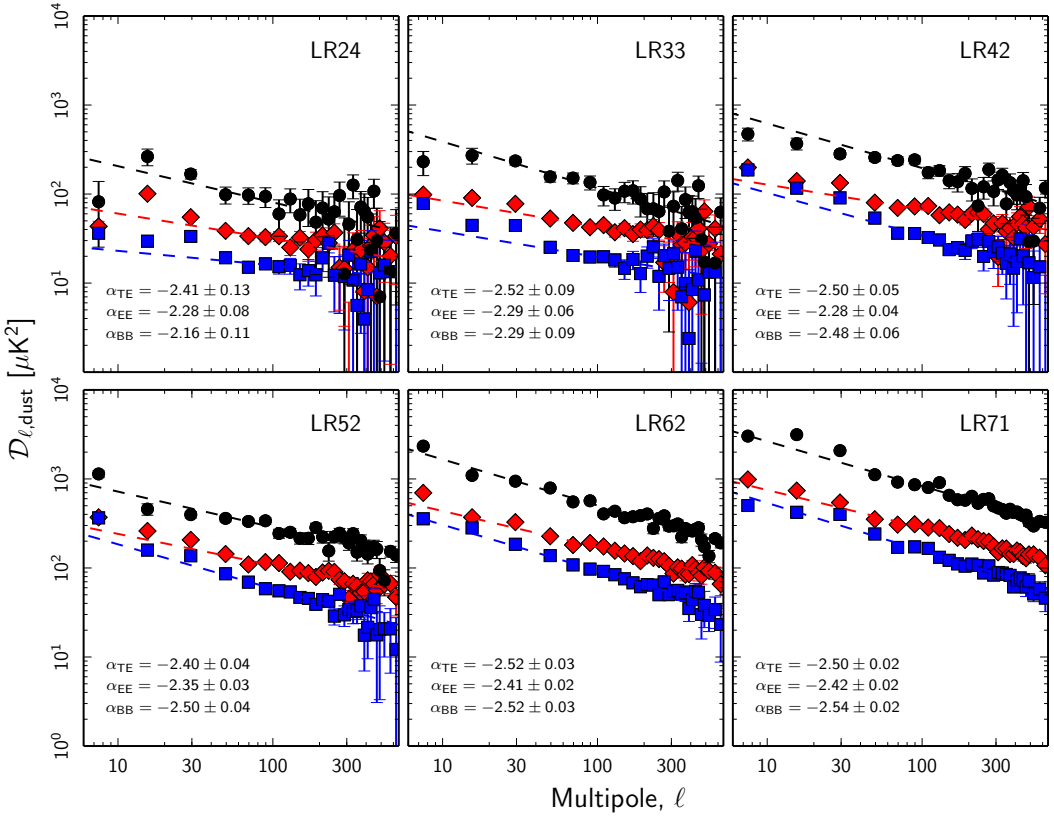

- The power-law exponents for ***EE*** and ***BB*** are slightly different
- Spectra are not well fitted by a single power- law over the full multipole-range
- The ***E/B*** asymmetry and ***T-E*** correlation extend to low multipoles

Planck 2018 results: *T-B* correlation

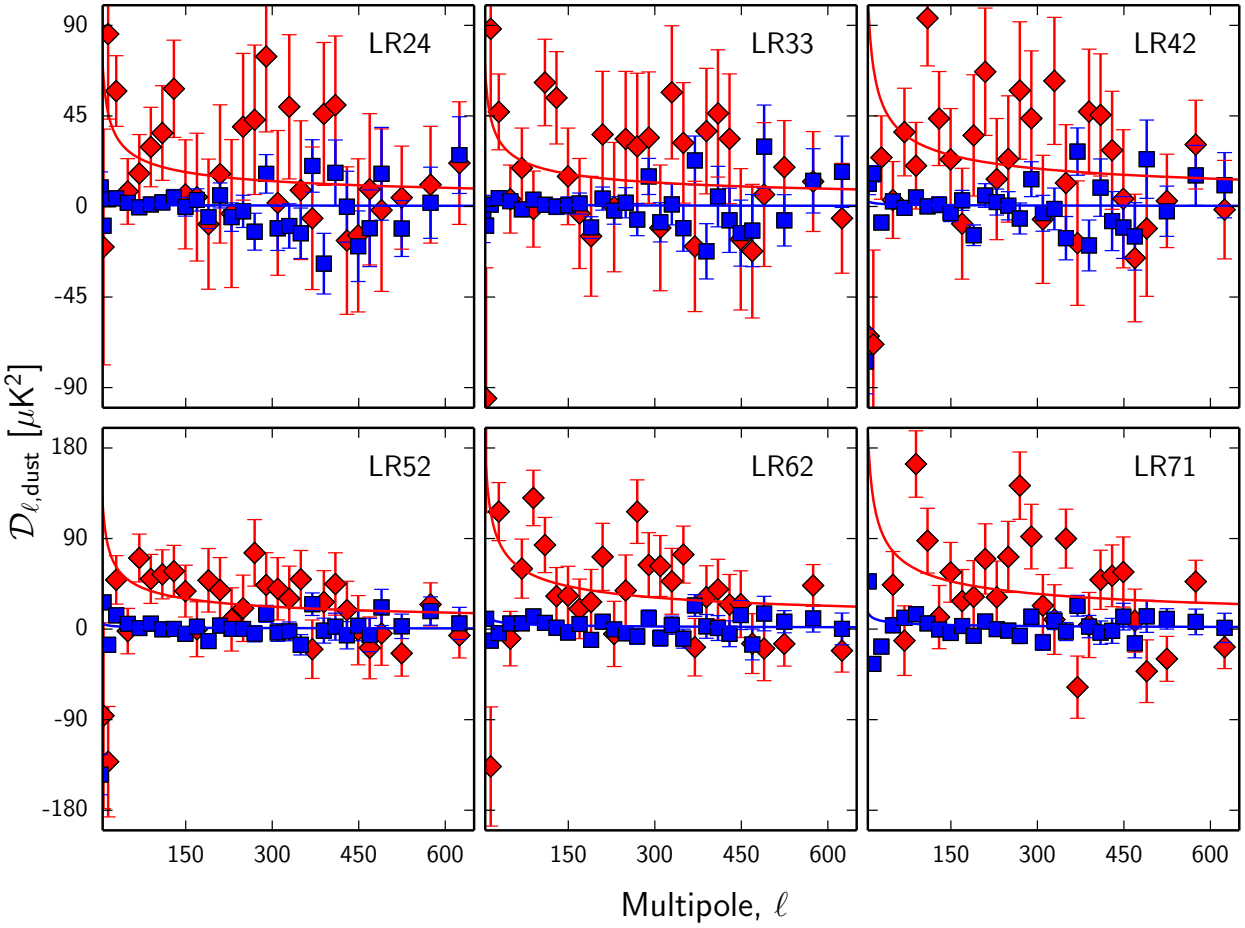

- Evidence for positive ***T-B*** correlation
- This result has not yet received an astrophysical interpretation
- Non-zero dust ***T-B*** could have an impact on experiments calibrating the absolute polarization angle by minimizing this quantity

353 GHz emission stacks

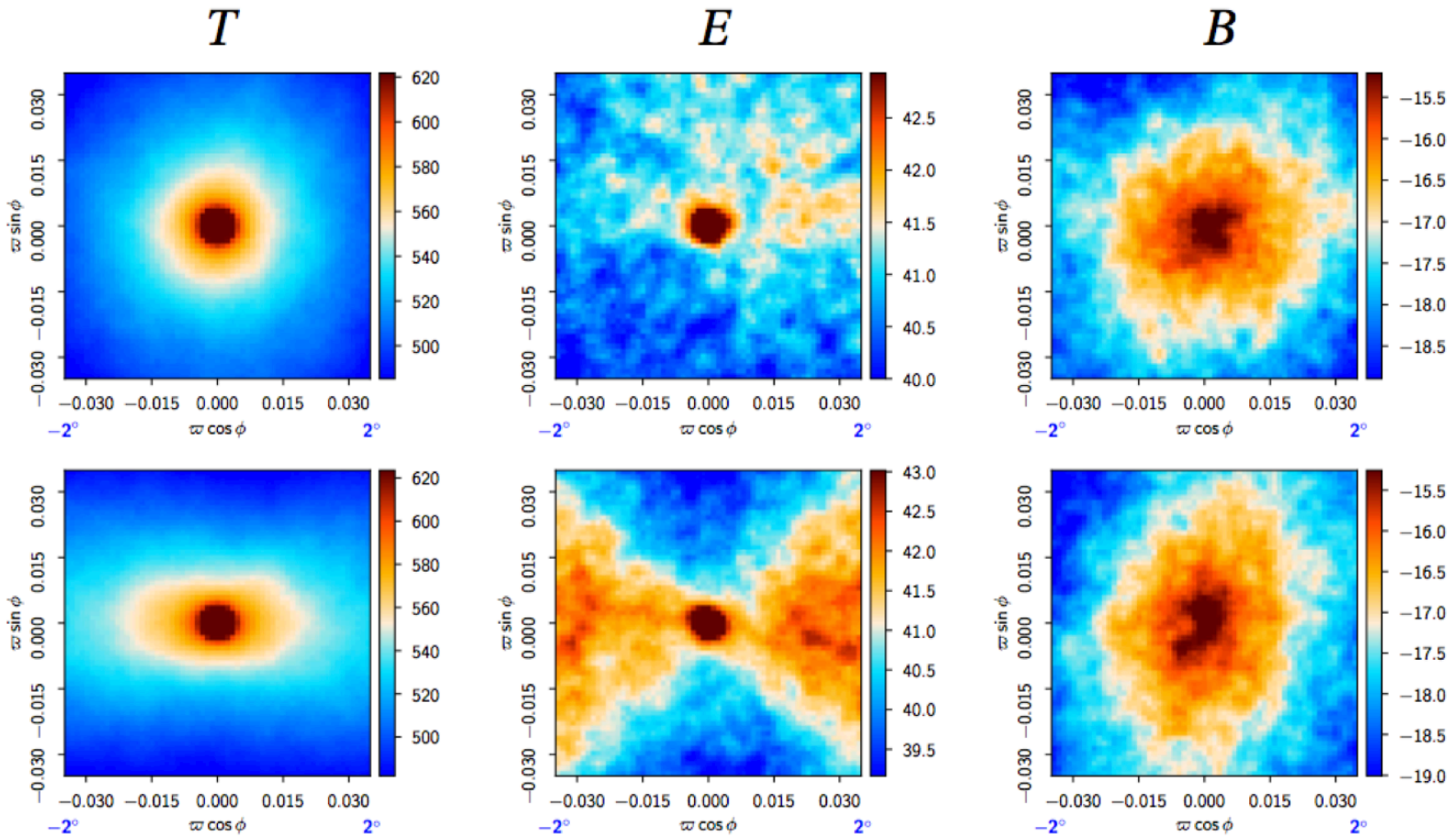

- Evidence for positive ***T*-*B*** correlation
- This result has not yet received an astrophysical interpretation
- Non-zero dust ***T*-*B*** could have an impact on experiments calibrating the absolute polarization angle by minimizing this quantity

Planck 2018 results VII

CMB emission stacks

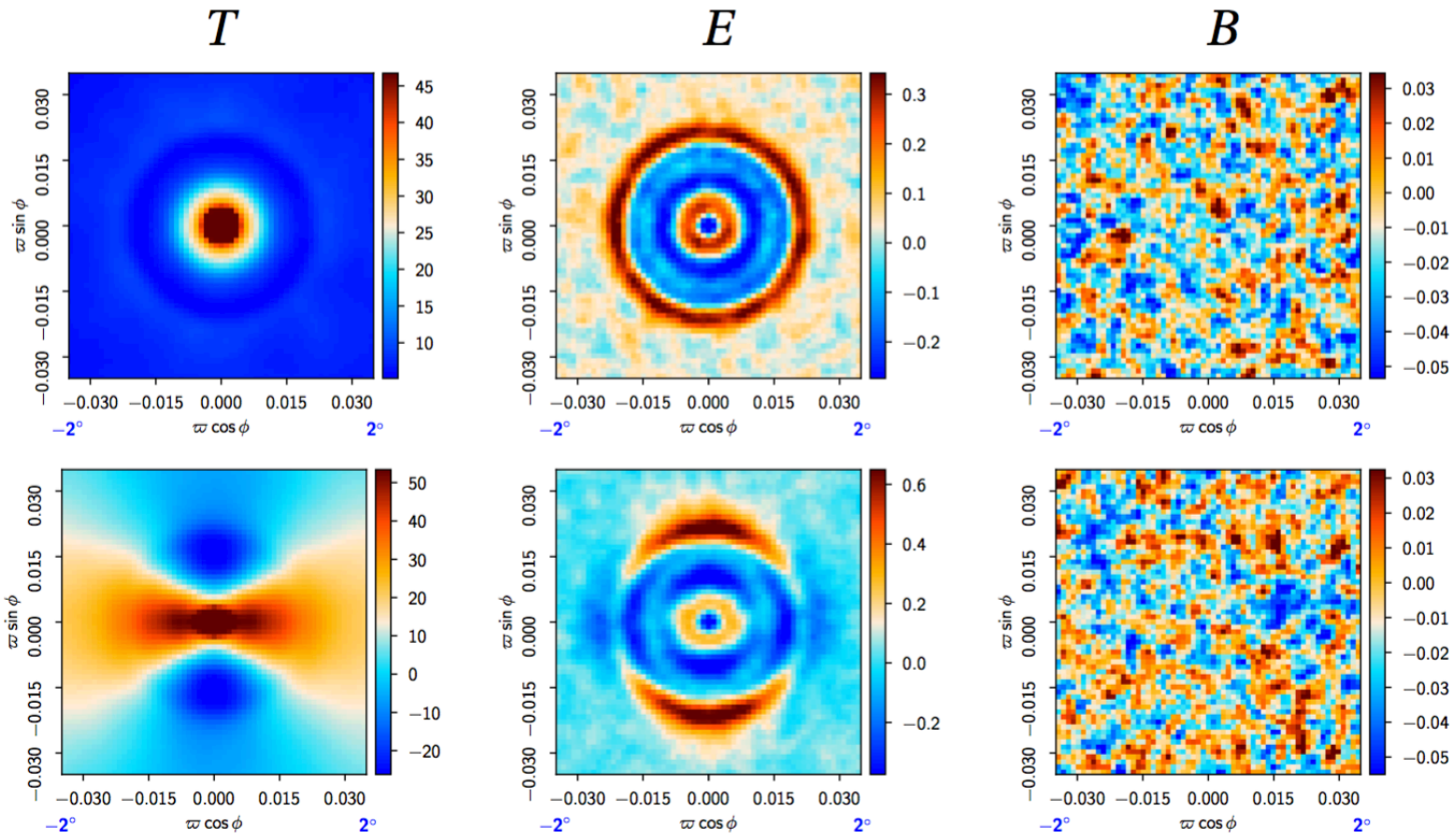

Planck 2018 results VII

Planck 2018 results: power scaling

- ***BB*** power well fitted by $(I_{353})^2$
- BICEP region's Planck dust ***BB*** power is compatible with (but lower than) the fit on larger masks

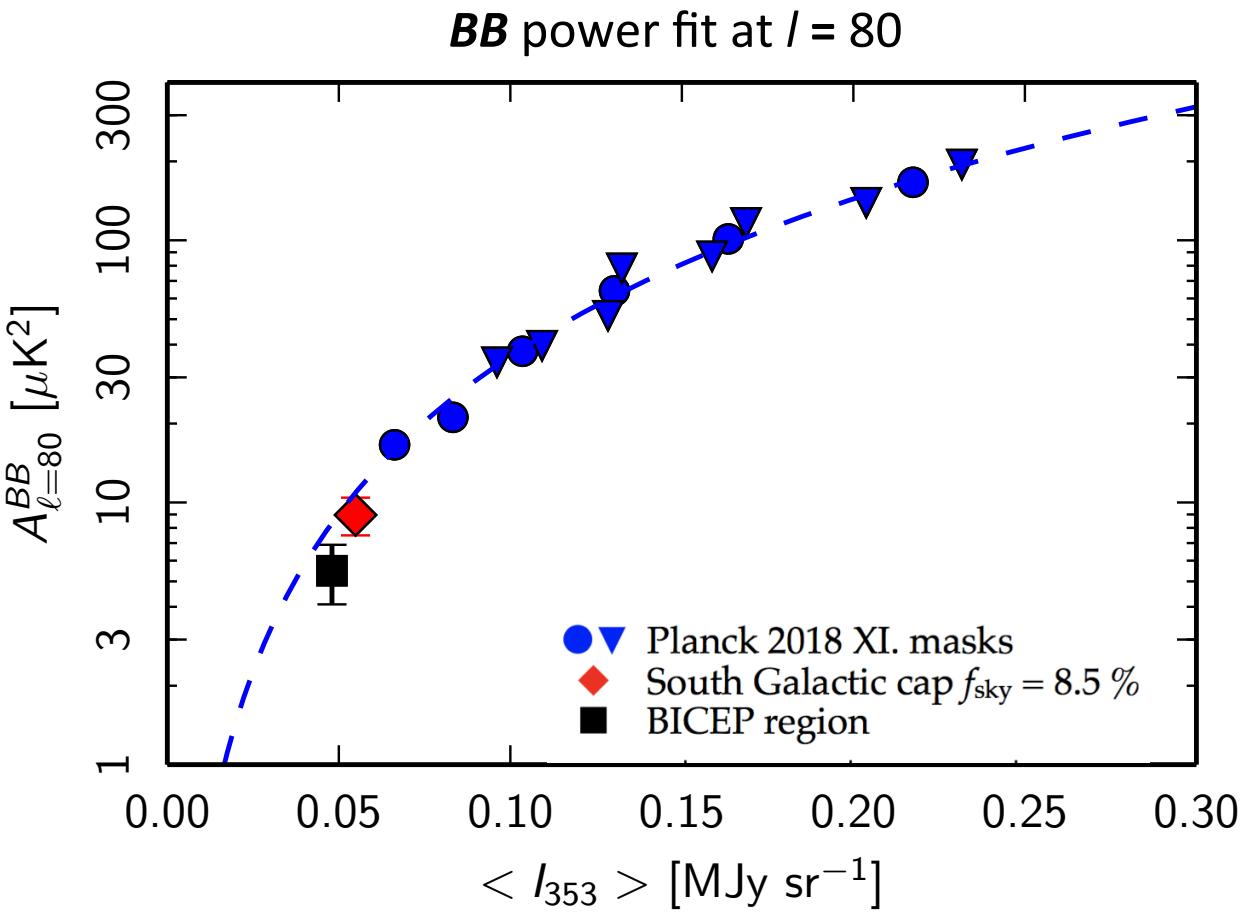

Multicomponent analysis in the harmonic space

- Divide the sky into six large sky regions (f_{sky}= 0.24, 0.33, 0.42, 0.52, 0.62 and 0.71).
- Compute auto- and cross-power spectra over all the sky regions using Xpol.
- CMB is removed from power spectra using the latest Planck best-fit model. CMB variance is included in the error-bars.
- Fit all the spectra simultaneously with five-parameter foreground model as a function of sky regions and multipoles.

foreground model = dust + synchrotron

amplitudes, spectral indices $A_{\rm d}, \beta_{\rm d}$ $A_{\rm s}, \beta_{\rm s}$

Dust-synchrotron correlation parameter = ρ

Spectral energy distribution of polarized foregrounds

To characterize the SED of polarized foregrounds, we combine the four lowest *Planck* HFI frequency channels (100 – 353 GHz) + LFI (30 GHz) + *WMAP* (23 and 33 GHz).

Amplitude of cross-spectra between frequencies ν_1 and ν_2 :

$$\mathcal{D}_\ell(\nu_1 \times \nu_2) = A_{\rm s} \left(\frac{\nu_1\nu_2}{28.4^2}\right)^{\beta_{\rm s}} + A_{\rm d} \left(\frac{\nu_1\nu_2}{353^2}\right)^{\beta_{\rm d}-2} \frac{B_{\nu_1}(T_{\rm d})}{B_{353}(T_{\rm d})} \frac{B_{\nu_2}(T_{\rm d})}{B_{353}(T_{\rm d})}$$
$$+ \rho\sqrt{A_{\rm s}A_{\rm d}} \left[\left(\frac{\nu_1}{28.4}\right)^{\beta_{\rm s}} \left(\frac{\nu_2}{353}\right)^{\beta_{\rm d}-2} \frac{B_{\nu_2}(T_{\rm d})}{B_{353}(T_{\rm d})} \right.$$
$$\left. + \left(\frac{\nu_2}{28.4}\right)^{\beta_{\rm s}} \left(\frac{\nu_1}{353}\right)^{\beta_{\rm d}-2} \frac{B_{\nu_1}(T_{\rm d})}{B_{353}(T_{\rm d})} \right] \qquad T_{\rm d} = 19.6\,{\rm K}$$

This model does not include spectral decorrelation.

Five model parameters:

- The synchrotron and dust amplitudes $A_{\rm s}$ and $A_{\rm d}$.
- The two spectral indices $\beta_{\rm s}$ and $\beta_{\rm d}$.
- The dust/synchrotron polarization correlation parameter ρ .

Choi and Page, astro-ph/1509.05934

Data fitting

- Auto- and cross-spectra of seven frequencies provide 28 data points.
- Error-bars on data points are derived from E2E simulations.
- CMB is removed from power spectra using the latest Planck best-fit model. CMB variance is included in the error-bars.
- Fit is done in two steps:
  - first step no prior.
  - second step, a prior, inferred from the results of the first fit, is introduced on the synchrotron spectral index ($\beta_{\rm s} = -3.13 \pm 0.07$).
- Same method repeated on the data, simulations are used to propagate the error-bars and check for a potential bias on foreground parameters.

LR62 BB spectra

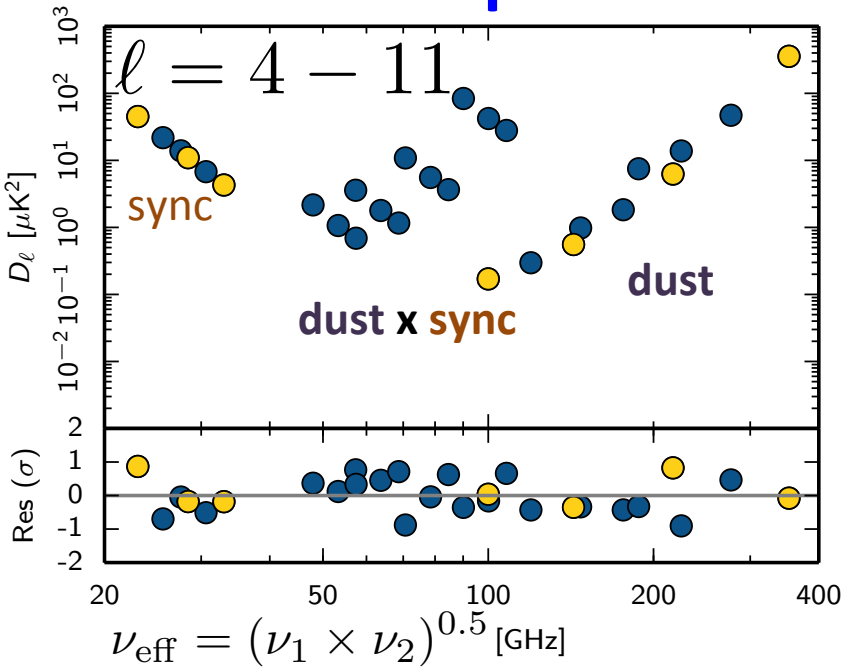

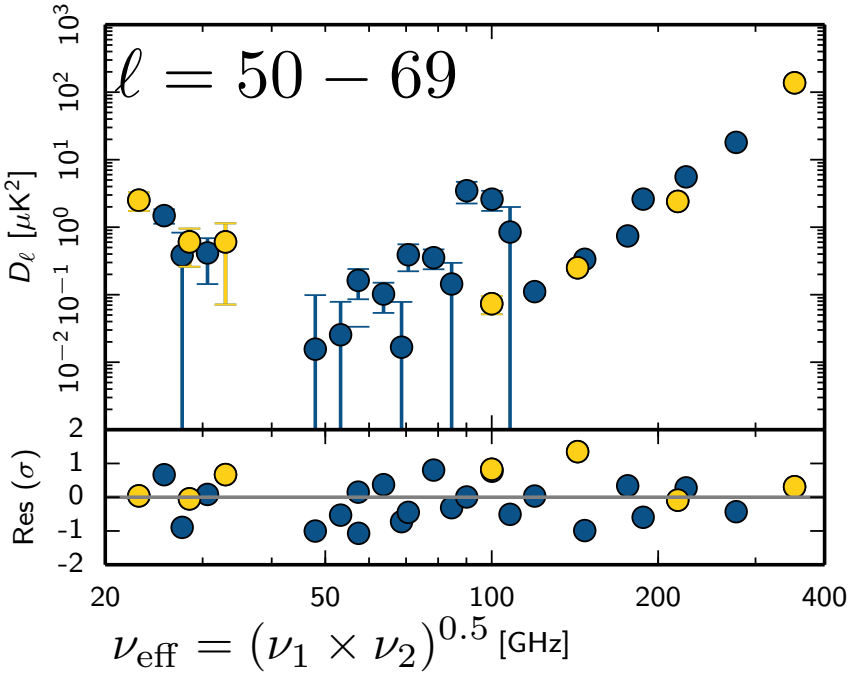

Illustration of data input and fit results

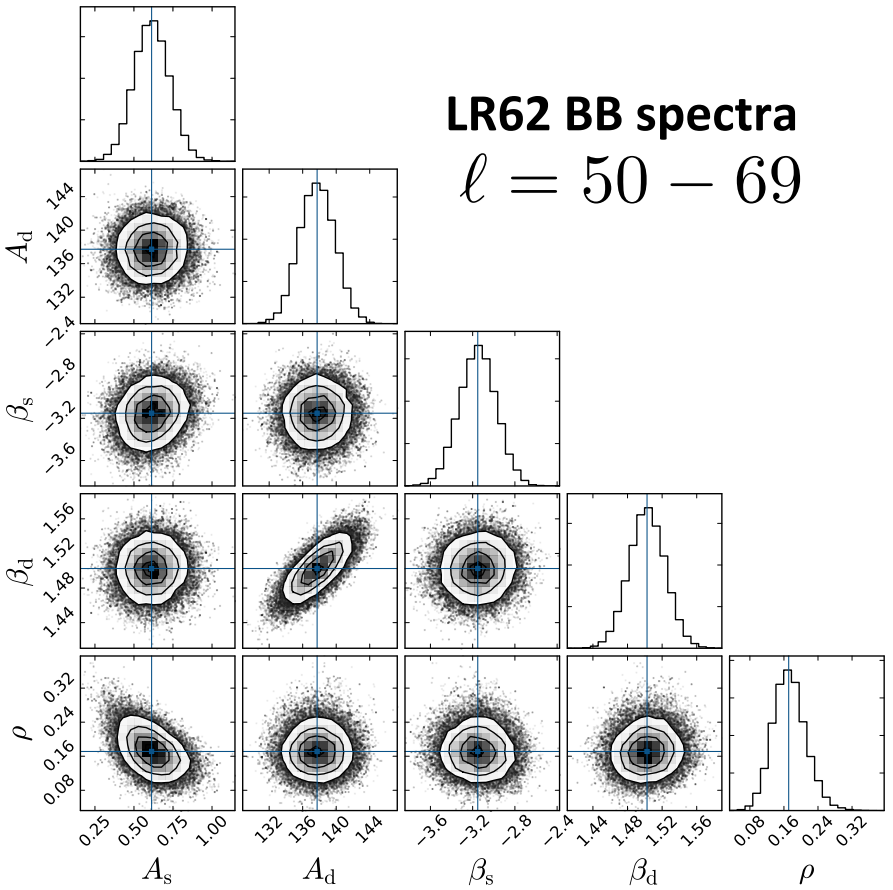

Dust and synchrotron spectral parameters

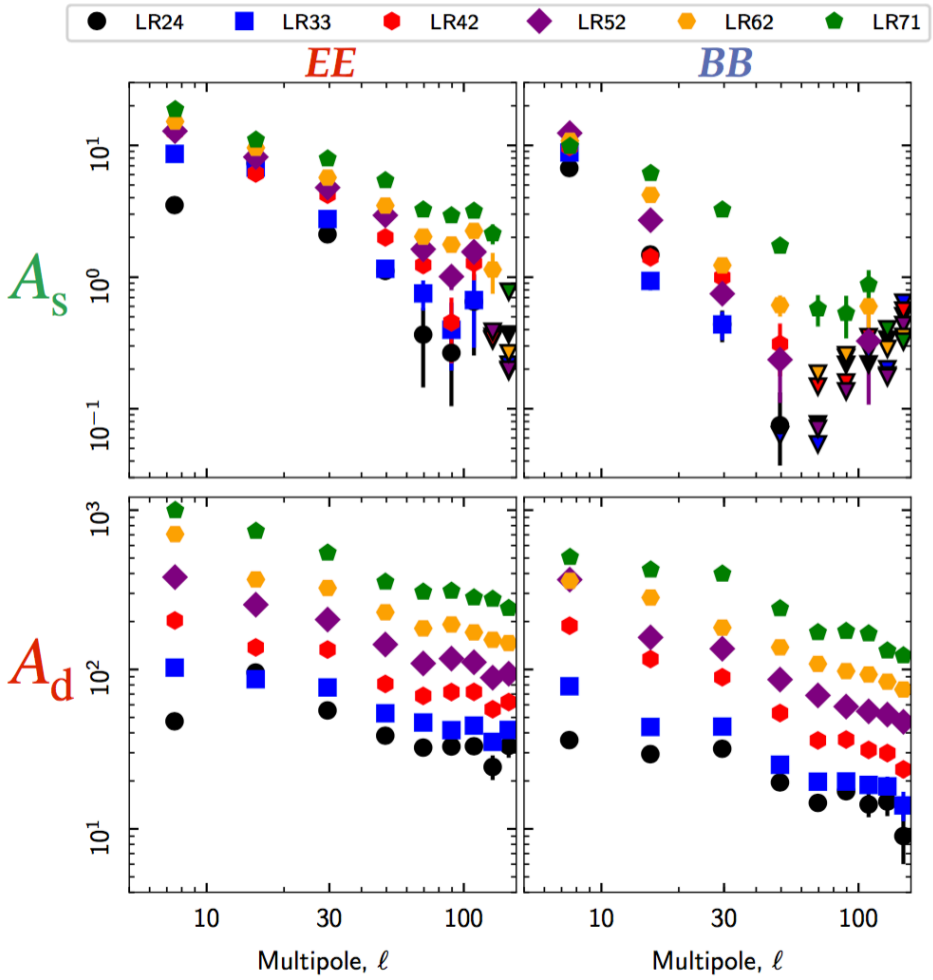

Inverted triangles = one sigma upper limit

BB A_s/A_d ratio is maximum at low multipoles
and for the smallest sky region (LR24)

Dust and synchrotron spectral parameters

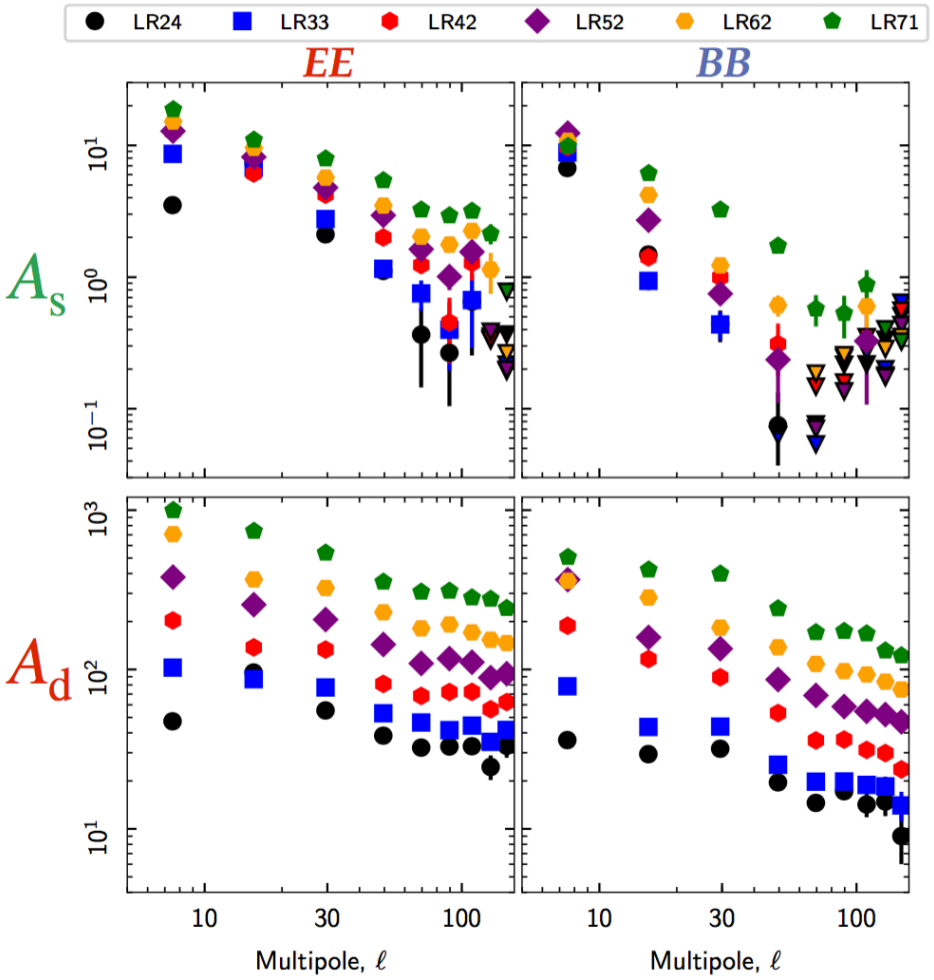

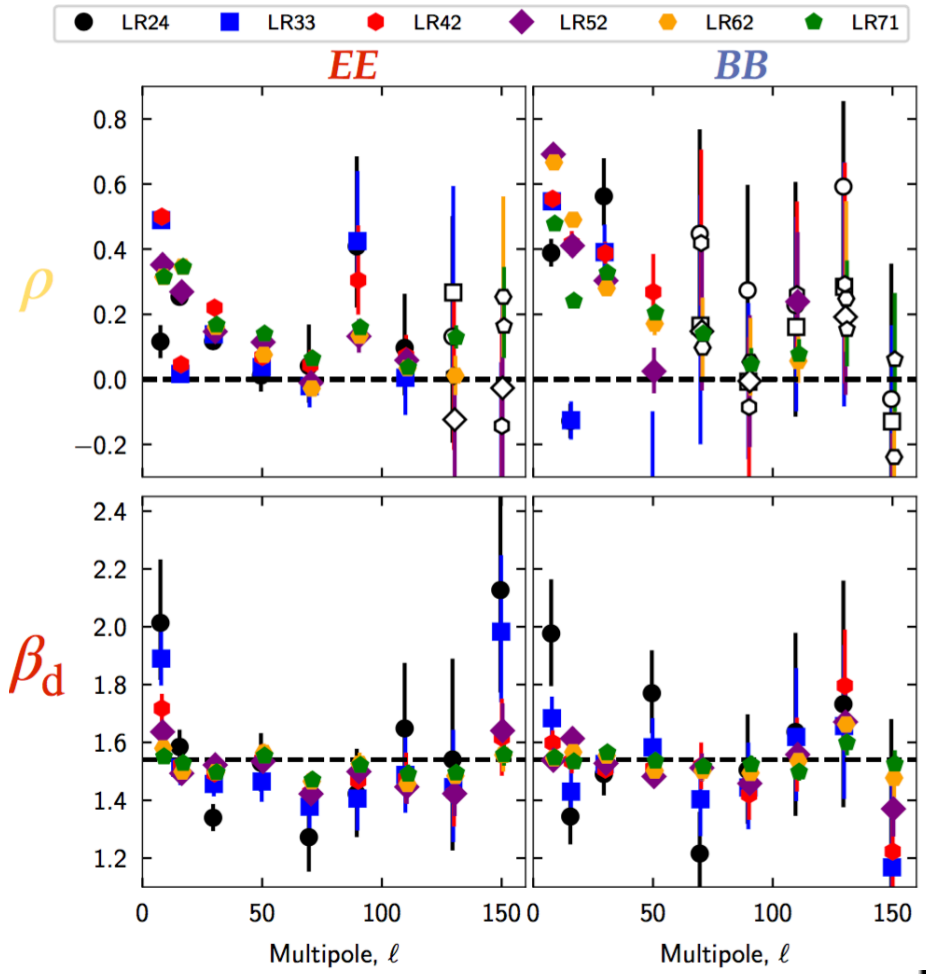

Inverted triangles = one sigma upper limit

BB A_s/A_d ratio is maximum at low multipoles and for the smallest sky region (LR24)

- Significant dust-synchrotron correlation at $l \lesssim 50$
- No evidence for dust spectral index l dependence

Dust spectral energy distribution

Dust SED in polarization

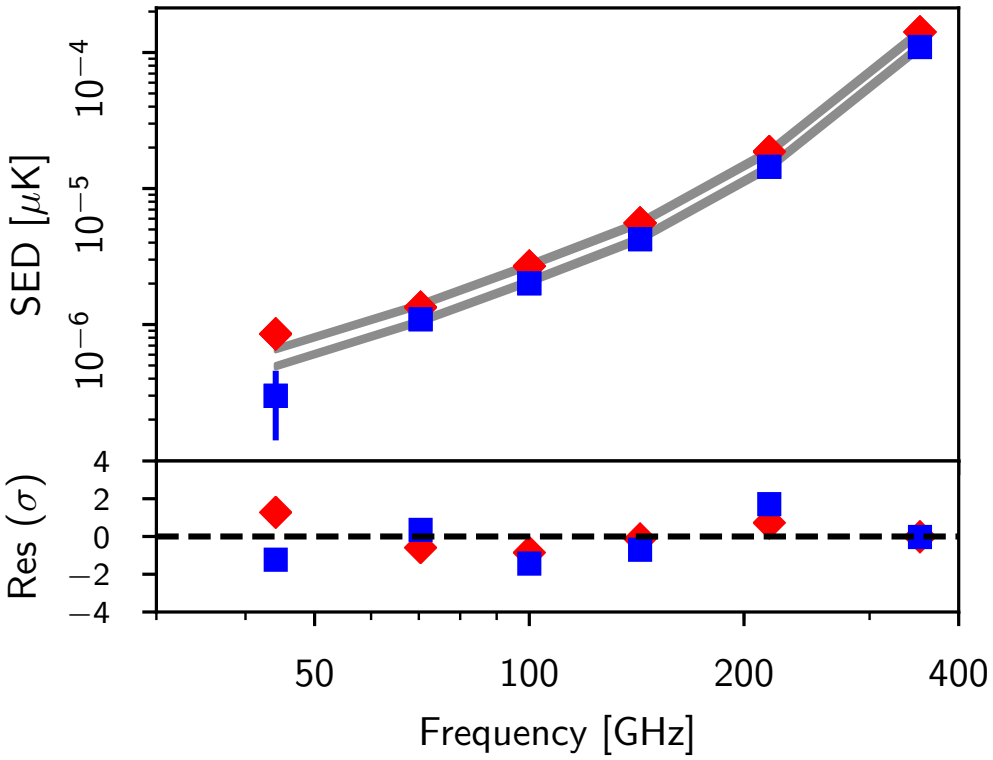

- In polarization, the dust SED from SMICA component separation method fits well by a single temperature modified black-body emission law from 353 GHz to 44 GHz.

Polarization vs total intensity

- The difference between spectral indices for polarization and total intensity is small (0.05 ± 0.03) and not of high statistical significance
- Planck data analysis suggests that the emission from a single grain type dominates the long-wavelength emission in both polarization and total intensity.

Reionization B-modes ℓ range

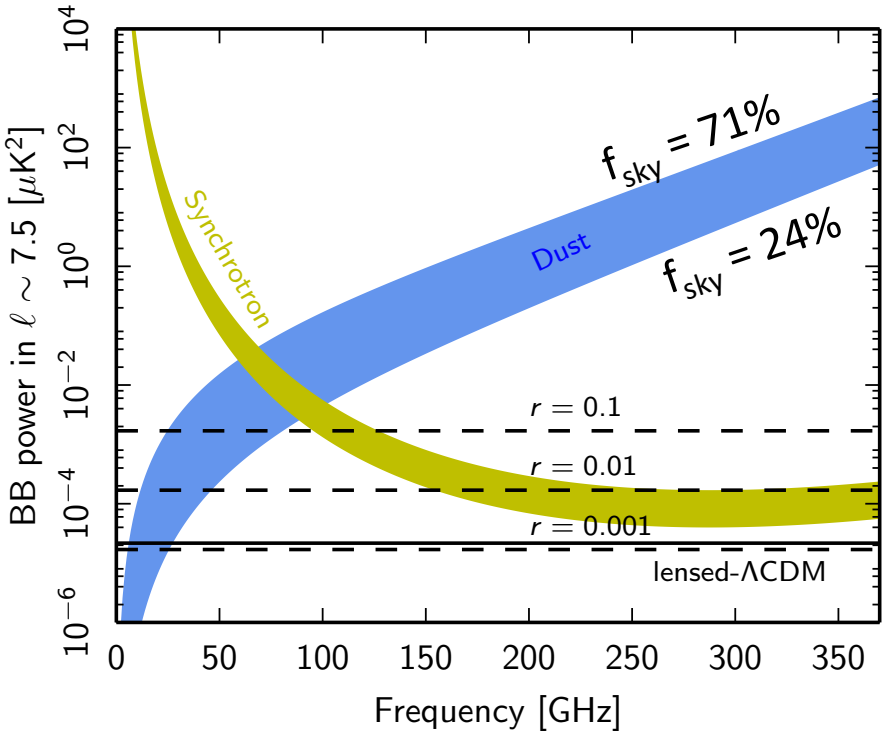

Recombination B-modes ℓ range

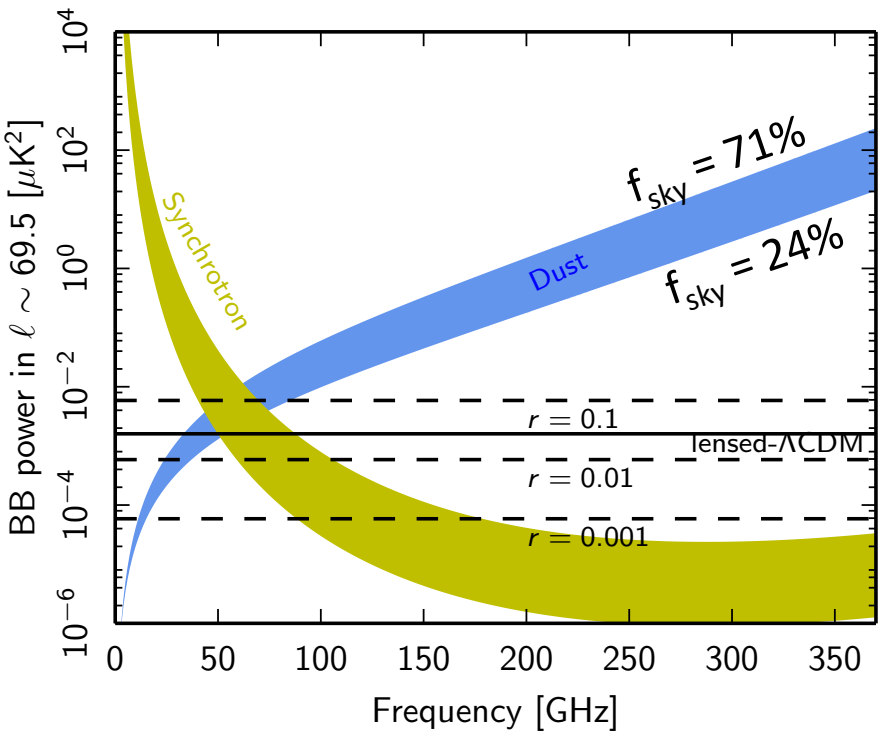

- The frequency at which dust and synchrotron *B*-modes power are equal depends on multipole and sky region.

- Dust quickly dominates synchrotron at higher frequencies.

Spectral energy distribution of dust emission

To characterize the spectral decorrelation of dust B-modes over the multipole bin 50-160, we only consider the four lowest *Planck* HFI frequency channels (100 – 353 GHz)

Amplitude of cross-spectra between HFI frequencies ν_1 and ν_2 :

$$\mathcal{D}_\ell(\nu_1 \times \nu_2) = A_{\rm d} \left(\frac{\nu_1 \nu_2}{353^2}\right)^{\beta_{\rm d}-2} \frac{B_{\nu_1}(T_{\rm d})}{B_{353}(T_{\rm d})} \frac{B_{\nu_2}(T_{\rm d})}{B_{353}(T_{\rm d})} R_\ell(\delta_{\rm d}, \nu_1, \nu_2)$$

where

$$R_\ell(\delta_{\rm d}, \nu_1, \nu_2) = \exp\left[-\delta_{\rm d} \ln\left(\frac{\nu_1}{\nu_2}\right)^2\right]$$

$$T_{\rm d} = 19.6\,{\rm K}$$

Assumes a frequency dependence model of spectral decorrelation based on ***Vansyngel et al. 2017***.

Three model parameters:

- The dust amplitude $A_{\rm d}$.
- The dust spectral index $\beta_{\rm d}$.
- The dust decorrelation parameter $\delta_{\rm d}$.

Dust frequency correlation

Frequency decorrelation due to effective SED spatial variations has to appear at some level

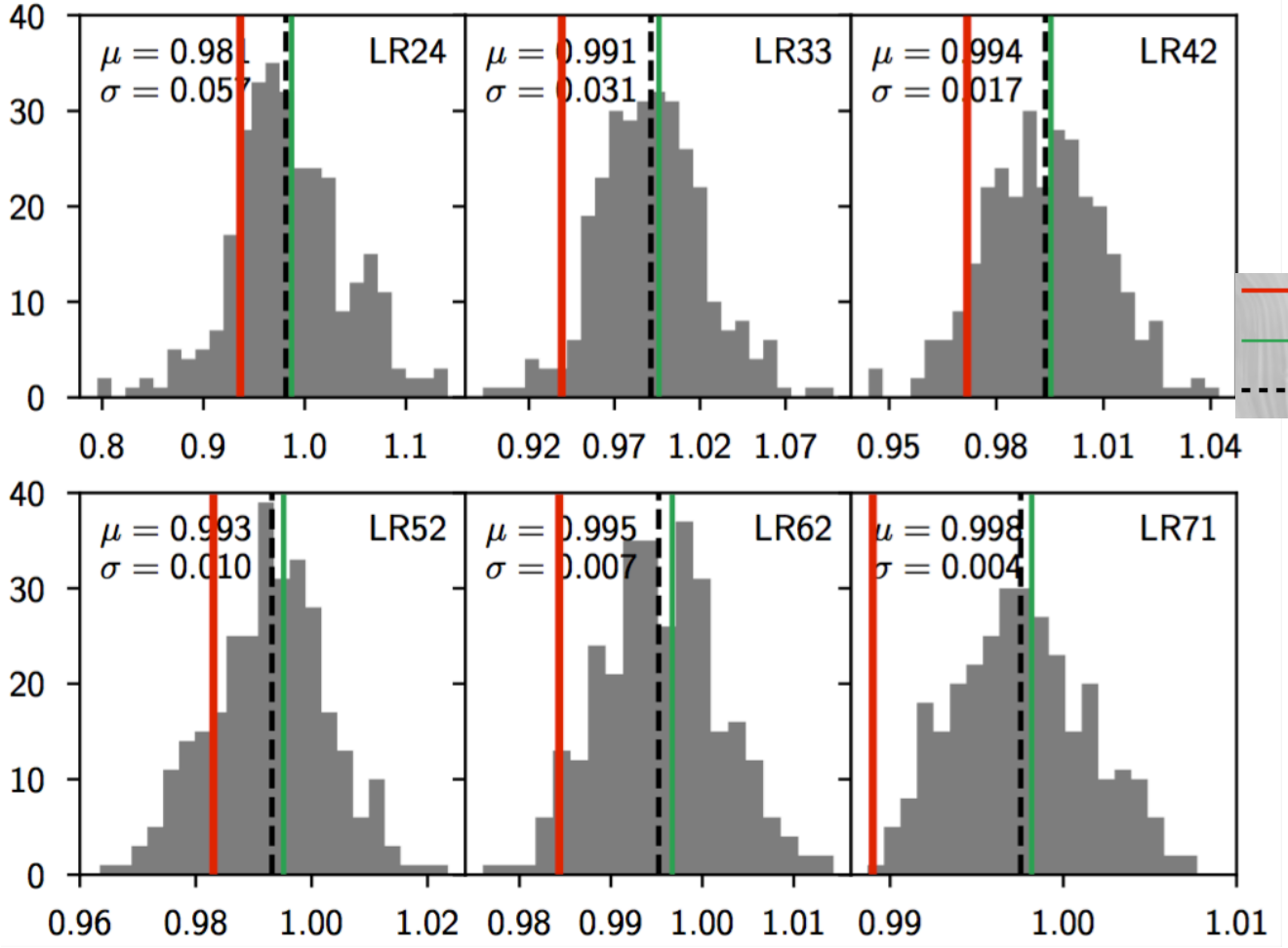

- results of HFI-only (100 – 353 GHz) multi-frequency fit over the multipole range 50 – 160.
- The mean of spectral correlation ratio is consistent with one within 1 sigma error-bars.

Averaging dust SEDs

Modified black body $I_\nu \propto \nu^\beta B_\nu(T)$

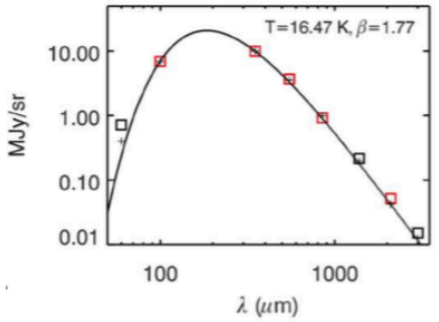

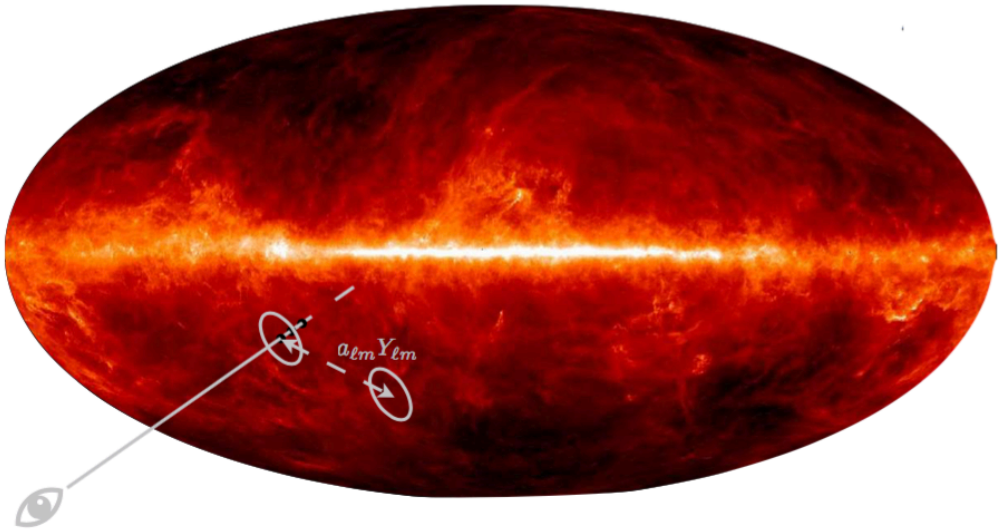

[Planck 2018 IV]

Modified black-body SED in *every* volume element

- ★ Line-of-sight average (*always there*!)
- ★ Experimental beam and frequency average
- ★ Map operations average (e.g., spherical harmonic expansion)

$$I_\nu \propto \nu^{\beta(\mathbf{n})} B_\nu(T(\mathbf{n}))$$

Dust SED spatial variations

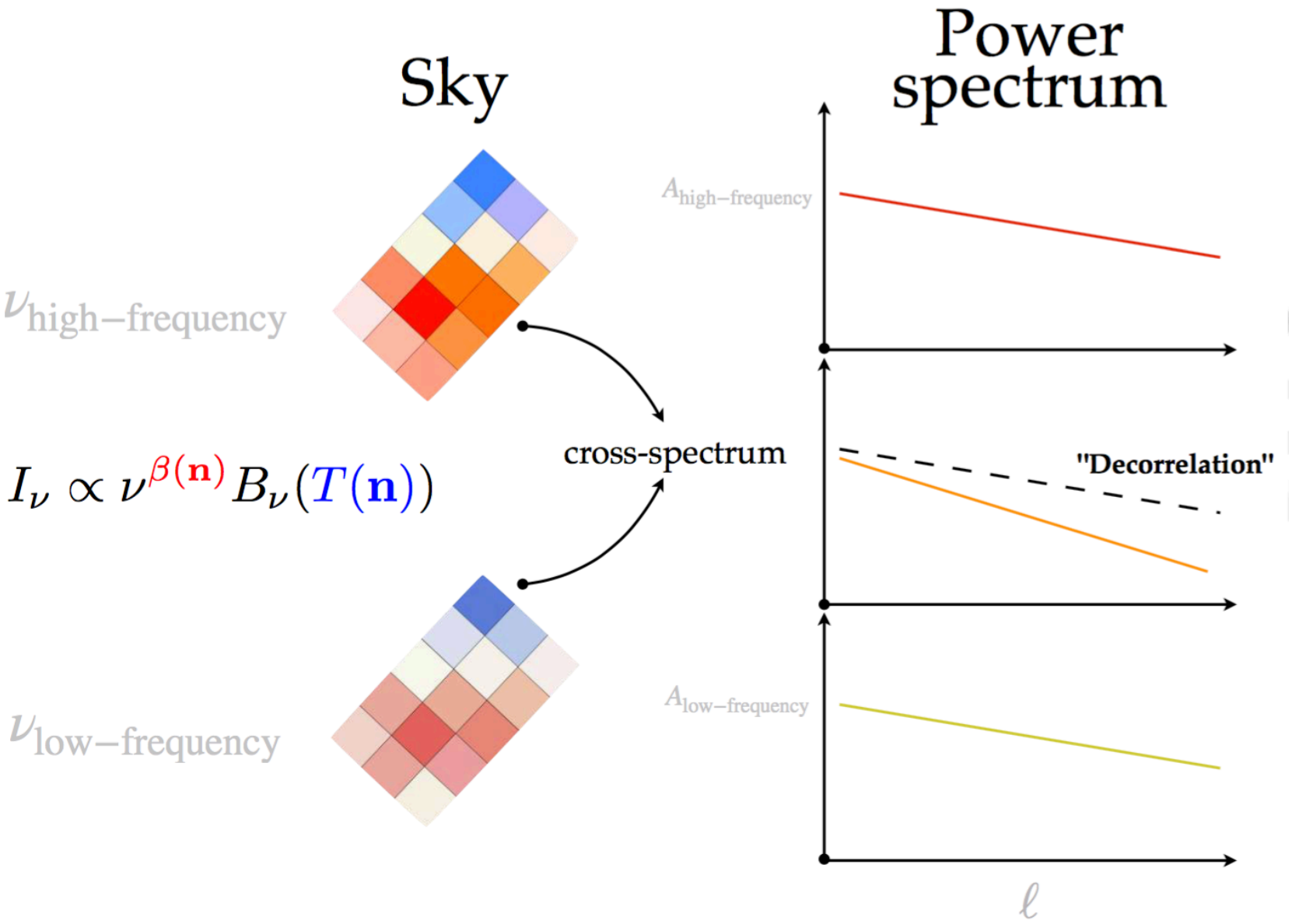

$$I_\nu \propto \nu^{\beta(\mathbf{n})} B_\nu(T(\mathbf{n}))$$

Spatial variations of the spectral behavior of polarized dust emission are a critical issue for the analysis of the CMB B-modes.

Problem : we do not know how to model the effective SED

Proposed solution : **MOMENT EXPANSION OF THE DUST SED**

* At the map level : [Chluba et al. (2017)]
* At the spectra level : [Mangilli et al. in prep. (2019)]

Dust: Moment expansion at the map level

$$I_\nu \propto \nu^{\beta(\mathbf{n})} B_\nu(T(\mathbf{n}))$$

$$I_\nu\left(p\left(\vec{n}_i\right)\right) + I_\nu\left(p\left(\vec{n}_j\right)\right) + \dots$$

Line-of-sight, beam or spherical harmonics average

Moment expansion of the SED

$$\begin{aligned}\langle I_\nu(\mathbf{p})\rangle = {} & I_\nu(\bar{\mathbf{p}}) \\ & + \sum_i \omega_i \partial_{p_i} I_\nu(\bar{\mathbf{p}}) \\ & + \frac{1}{2}\sum_{ij} \omega_{ij} \partial_{p_i}\partial_{p_j} I_\nu(\bar{\mathbf{p}}) \\ & + \frac{1}{6}\sum_{ijk} \omega_{ijk} \partial_{p_i}\partial_{p_j}\partial_{p_k} I_\nu(\bar{\mathbf{p}}) \\ & + \dots\end{aligned}$$

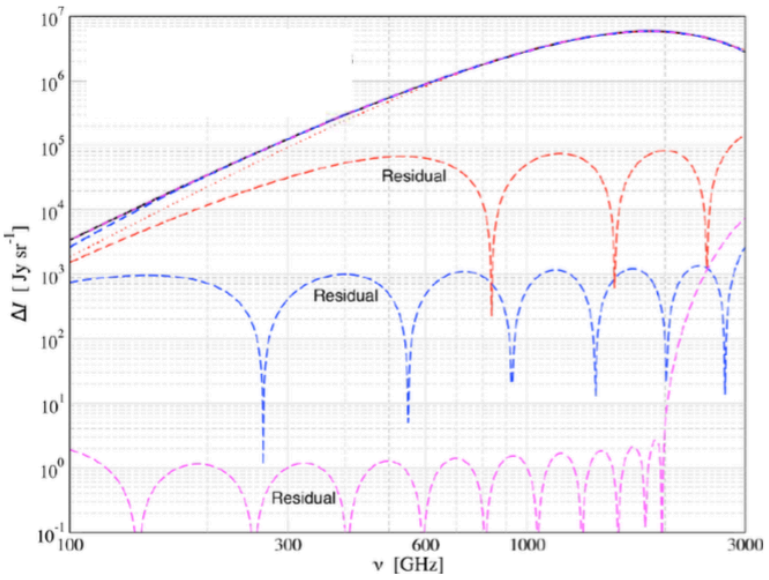

[Chluba et al., 2017]

BICEP-KECK 2015 results

r < 0.07
(95% CL)

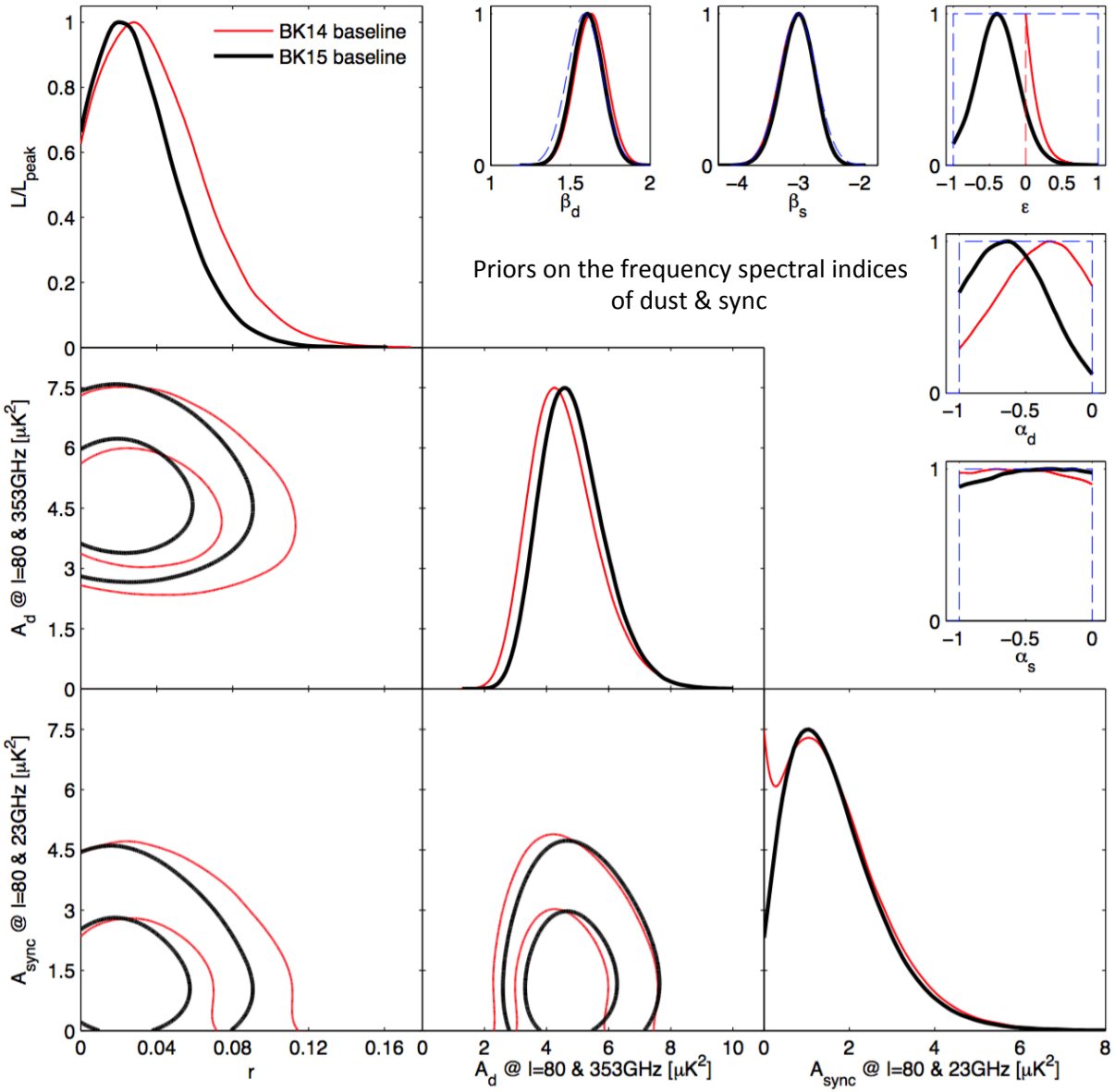

Priors on the frequency spectral indices of dust & sync

Dust – synchrotron correlation

Marginalize over generous ranges in spatial spectral indices

Weak detection of synchrotron emission

BK-X 2018 results

BK15 results

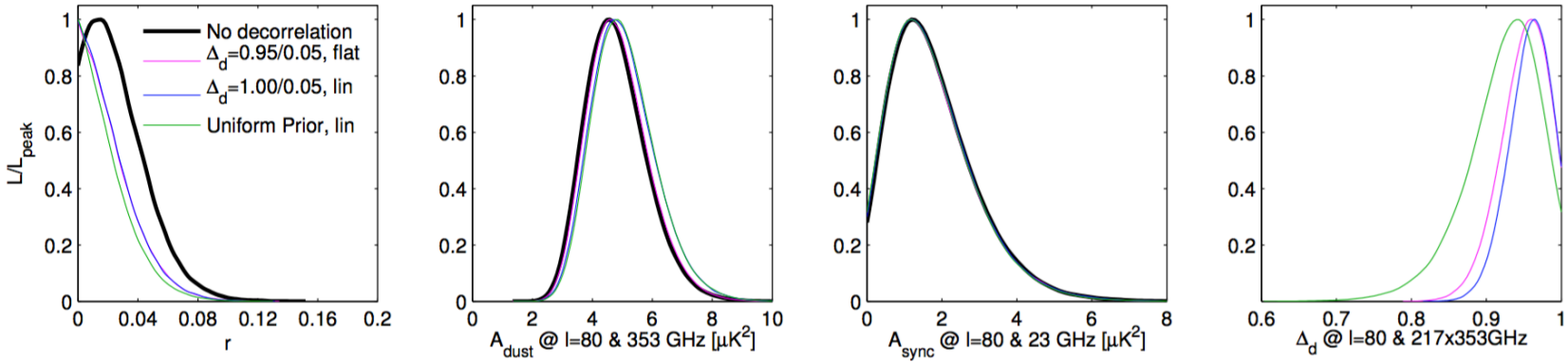

Likelihood results when including the dust decorrelation parameter

Summary

Planck has provided the observational inputs needed to understand and model Galactic polarized foregrounds for preparing future experiments, and optimizing and assessing component separations

- Dust polarization power spectra measured down to the lowest multipoles
- Spectral model of the polarized foregrounds including dust-synchrotron correlation
- Upper limits on frequency decorrelation of dust polarization